



Mobility & Vehicle Mechanics

*International Journal for Vehicle Mechanics, Engines and
Transportation Systems*

ISSN 1450 - 5304

UDC 621 + 629(05)=802.0

Pikula Boran Trobradović Mirsad	CONTRIBUTION TO THE DEFINITION OF THE MOST IMPORTANT PARAMETERS FOR TIRE MODELS	7-18
Dejanu Marcel , Popa Dinel, Dascălu Traian, Tabacu Ion, Pârlac Sebastian	EXPERIMENTAL BENCH FOR RECORDING IMAGES OF THE FLAME FRONT WHEN USING LASER PLUG IGNITION	19-29
Catalin Zaharia, Adrian Clenci	RESEARCHES ON THE IMPACT OF HYPERMILING TECHNIQUES AND FUEL SAVING DEVICES IN ORDER TO REDUCE POLLUTION IN URBAN AREAS	31-42
Dobrivoje Ninković, Dragan Taranović, Saša Milojević, Radivoje Pešić	IMODELLING VALVE DYNAMICS AND FLOW IN RECIPROCATING COMPRESSORS	45-63



M V M

Mobility Vehicle Mechanics

Editors: Prof. dr Jovanka Lukić; Prof. dr Čedomir Duboka

MVM Editorial Board
University of Kragujevac
Faculty of Engineering
Sestre Janjić 6, 34000 Kragujevac, Serbia
Tel.: +381/34/335990; Fax: + 381/34/333192

Prof. Dr **Belingardi Giovanni**
Politecnico di Torino,
Torino, ITALY

Dr Ing. **Ćučuz Stojan**
Visteon corporation,
Novi Jicin,
CZECH REPUBLIC

Prof. Dr **Demić Miroslav**
University of Kragujevac
Faculty of Engineering
Kragujevac, SERBIA

Prof. Dr **Fiala Ernest**
Wien, OESTERREICH

Prof. Dr **Gillespie D. Thomas**
University of Michigan,
Ann Arbor, Michigan, USA

Prof. Dr **Grujović Aleksandar**
University of Kragujevac
Faculty of Engineering
Kragujevac, SERBIA

Prof. Dr **Knapezyk Josef**
Politechniki Krakowskiej,
Krakow, POLAND

Prof. Dr **Krstić Božidar**
University of Kragujevac
Faculty of Engineering
Kragujevac, SERBIA

Prof. Dr **Mariotti G. Virzi**
Universita degli Studidi Palermo,
Dipartimento di Meccanica ed
Aeronautica,
Palermo, ITALY

Prof. Dr **Pešić Radivoje**
University of Kragujevac
Faculty of Engineering
Kragujevac, SERBIA

Prof. Dr **Petrović Stojan**
Faculty of Mech. Eng. Belgrade,
SERBIA

Prof. Dr **Radonjić Dragoljub**
University of Kragujevac
Faculty of Engineering
Kragujevac, SERBIA

Prof. Dr **Radonjić Rajko**
University of Kragujevac
Faculty of Engineering
Kragujevac, SERBIA

Prof. Dr **Spentzas Constantinos**
N. National Technical University,
GREECE

Prof. Dr **Todorović Jovan**
Faculty of Mech. Eng. Belgrade,
SERBIA

Prof. Dr **Toliskyj Vladimir E.**
Academician NAMI,
Moscow, RUSSIA

Prof. Dr **Teodorović Dušan**
Faculty of Traffic and Transport
Engineering,
Belgrade, SERBIA

Prof. Dr **Veinović Stevan**
University of Kragujevac
Faculty of Engineering
Kragujevac, SERBIA

For Publisher: Prof. dr Miroslav Živković, dean, University of Kragujevac, Faculty of Engineering

***Publishing of this Journal is financially supported from:
Ministry of Education, Science and Technological Development, Republic Serbia***

MVM – International Journal for Vehicle Mechanics, Engines and Transportation Systems
NOTIFICATION TO AUTHORS

The Journal MVM publishes original papers which have not been previously published in other journals. This is responsibility of the author. The authors agree that the copyright for their article is transferred to the publisher when the article is accepted for publication.

The language of the Journal is English.

Journal *Mobility & Vehicles Mechanics* is at the SSCI list.

All submitted manuscripts will be reviewed. Entire correspondence will be performed with the first-named author.

Authors will be notified of acceptance of their manuscripts, if their manuscripts are adopted.

INSTRUCTIONS TO AUTHORS AS REGARDS THE TECHNICAL ARRANGEMENTS OF MANUSCRIPTS:

Abstract is a separate Word document, “*First author family name_ABSTRACT.doc*”. Native authors should write the abstract in both languages (Serbian and English). The abstracts of foreign authors will be translated in Serbian.

This document should include the following: 1) author’s name, affiliation and title, the first named author’s address and e-mail – for correspondence, 2) working title of the paper, 3) abstract containing no more than 100 words, 4) abstract containing no more than 5 key words.

The manuscript is the separate file, „*First author family name_Paper.doc*“ which includes appendices and figures involved within the text. At the end of the paper, a reference list and eventual acknowledgements should be given. References to published literature should be quoted in the text brackets and grouped together at the end of the paper in numerical order.

Paper size: Max 16 pages of B5 format, excluding abstract

Text processor: Microsoft Word

Margins: left/right: mirror margin, inside: 2.5 cm, outside: 2 cm, top: 2.5 cm, bottom: 2 cm

Font: Times New Roman, 10 pt

Paper title: Uppercase, bold, 11 pt

Chapter title: Uppercase, bold, 10 pt

Subchapter title: Lowercase, bold, 10 pt

Table and chart width: max 125 mm

Figure and table title: Figure _ (Table _): Times New Roman, italic 10 pt

Manuscript submission: application should be sent to the following e-mail:

mvm@kg.ac.rs ; lukicj@kg.ac.rs

or posted to address of the Journal:

University of Kragujevac – Faculty of Engineering

International Journal M V M

Sestre Janjić 6, 34000 Kragujevac, Serbia

The Journal editorial board will send to the first-named author a copy of the Journal offprint.

OBAVEŠTENJE AUTORIMA

Časopis MVM objavljuje originalne radove koji nisu prethodno objavljivani u drugim časopisima, što je odgovornost autora. Za rad koji je prihvaćen za štampu, prava umnožavanja pripadaju izdavaču.

Časopis se izdaje na engleskom jeziku.

Časopis *Mobility & Vehicles Mechanics* se nalazi na SSCI listi.

Svi prispeli radovi se recenziraju. Sva komunikacija se obavlja sa prvim autorom.

UPUTSTVO AUTORIMA ZA TEHNIČKU PRIPREMU RADOVA

Rezime je poseban Word dokument, „*First author family name_ABSTRACT.doc*“. Za domaće autore je dvojezičan (srpski i engleski). Inostranim autorima rezime se prevodi na srpski jezik. Ovaj dokument treba da sadrži: 1) ime autora, zanimanje i zvanje, adresu prvog autora preko koje se obavlja sva potrebna korespondencija; 2) naslov rada; 3) kratak sažetak, do 100 reči, 4) do 5 ključnih reči.

Rad je poseban fajl, „*First author family name_Paper.doc*“ koji sadrži priloge i slike uključene u tekst. Na kraju rada nalazi se spisak literature i eventualno zahvalnost. Numeraciju korišćenih referenci treba navesti u srednjim zagradama i grupisati ih na kraju rada po rastućem redosledu.

Dužina rada: Najviše 16 stranica B5 formata, ne uključujući rezime

Tekst procesor: Microsoft Word

Margine: levo/desno: mirror margine; unurašnja: 2.5 cm; spoljna: 2 cm, gore: 2.5 cm, dole: 2 cm

Font: Times New Roman, 10 pt

Naslov rada: Velika slova, bold, 11 pt

Naslov poglavlja: Velika slova, bold, 10 pt

Naslov potpoglavlja: Mala slova, bold, 10 pt

Širina tabela, dijagrama: max 125 mm

Nazivi slika, tabela: Figure __ (Table __): Times New Roman, italic 10 pt

Dostavljanje rada elektronski na E-mail: mvm@kg.ac.rs ; lukicj@kg.ac.rs

ili poštom na adresu Časopisa
Redakcija časopisa M V M
Fakultet inženjerskih nauka
Sestre Janjić 6, 34000 Kragujevac, Srbija

Po objavljivanju rada, Redakcija časopisa šalje prvom autoru jedan primerak časopisa.

Mobility &

Motorna

Vehicle

**Volume 39
Number 3
2013.**

Vozila i

Mechanics

Motori

Pikula Boran
Trobradović Mirsad

CONTRIBUTION TO THE DEFINITION
OF THE MOST IMPORTANT
PARAMETERS FOR TIRE MODELS

7-18

Dejanu Marcel , Popa
Dinel, Dascălu Traian,
Tabacu Ion, Pârlac
Sebastian

EXPERIMENTAL BENCH FOR
RECORDING IMAGES OF THE FLAME
FRONT WHEN USING LASER PLUG
IGNITION

19-29

Catalin Zaharia,
Adrian Clenci

RESEARCHES ON THE IMPACT OF
HYPERMILING TECHNIQUES AND
FUEL SAVING DEVICES IN ORDER TO
REDUCE POLLUTION IN URBAN
AREAS

31-42

Dobrivoje Ninković,
Dragan Taranović,
Saša Milojević,
Radivoje Pešić

MODELLING VALVE DYNAMICS AND
FLOW IN RECIPROCATING
COMPRESSORS

45-63

Mobility &

Motorna

Vehicle

**Volume 39
Number 3
2013.**

Vozila i

Mechanics

Motori

Pikula Boran Trobradović Mirsad	PRILOG DEFINISANJU NAJZNAČAJNIJIH PARAMETARA MODELA PNEUMATIKA	7-18
Dejanu Marcel , Popa Dinel, Dascălu Traian, Tabacu Ion, Pârlac Sebastian	EKSPERIMENTALNI MOST ZA SNIMANJE PLAMENOG FRONTA KORIŠĆENJEM LASERSKOG PALJENJA	19-29
Catalin Zaharia, Adrian Clenci	RESEARCHES ON THE IMPACT OF HYPERMILING TECHNIQUES AND FUEL SAVING DEVICES IN ORDER TO REDUCE POLLUTION IN URBAN AREAS	31-42
Dobrivoje Ninković, Dragan Taranović, Saša Milojević, Radivoje Pešić	MODELIRANJE DINAMIKE VENTILA I PROTOKA U KLIPNIM KOMPRESORIMA	45-63

CONTRIBUTION TO THE DEFINITION OF THE MOST IMPORTANT PARAMETERS FOR TIRE MODELS

Pikula Boran¹, Trobradović Mirsad

UDC: 629.1;519.657

ABSTRACT: A modern development of motor vehicles, especially in the field of active safety, is impossible to image without prediction of adhesion in the contact between tire and road in any kind of vehicle dynamics simulation. There were a great number of different tire models during the history, from analytic expressions based on experimental results to semi empirical and physical models. The first ones, like Pacejka, etc. achieve excellent results, thanks to approximation based on the experimental results, that are valuable only for one tire in specific experimental conditions. On the other hand, physical models have major problem in definition of influenced parameters and knowing exact values, mostly in function of some influenced parameters.

Having in mind all mentioned facts, the paper is objected to the analysis of existing tire models and improvements in definition the most important parameters in some physical models. Based on the experimental results, the most important parameters in tire modeling are defined, especially tire stiffness, friction and adhesion coefficient in function of vertical load and longitudinal and lateral slip. Finally, the comparison between different tire models are shown and the best tire models recommended for simulations in the future

KEYWORDS: tire, tire model, vehicle simulation

PRIOLOG DEFINISANJU NAJVAŽNIJIH PARAMETARA MODELA PNEUMATIKA

REZIME: Savremeni razvoj motornih vozila, naročito u oblasti aktivne bezbednosti vozila, nemoguće je zamisliti bez predviđanja prijanjanja u zoni kontakta pneumatika i podloge u procesu simulacije dinamike vozila. Postoji značajan broj različitih modela pneumatika razvijenih tokom vremena, počev od analitičkih zasnovanih na eksperimentalnim rezultatima do polu empirijskih i fizičkih modela. Prvi, na primer kao Pacejkin model, daje odlične rezultate, jer aproksimacija modela analitičkim izrazom formirana na osnovu eksperimentalnih rezultata, koji su validni samo u specifičnim eksperimentalnim uslovima. Sa druge strane, fizički modeli imaju problem pri definisanju uticajnih parametara i poznavanju konkretnih vrednosti uglavnom u funkciji nekih uticajnih parametara.

Imajući prethodno u vidu, cilj rada je analiza postojećih modela pneumatika i poboljšanje u definisanju najuticajnih parametara kod nekih fizičkih modela. Na osnovu eksperimentalnih rezultata, najvažniji parametri kod modeliranja pneumatika su definisani, naročito krutost pneumatika, koeficijenti trenja i prijanjanja u funkciji vertikalnog opterećenja i podužnog i bočnog klizanja. Konačno, uporedna analiza različitih modela je prikazana u radu i date su preporuke za izbor simulacionog modela u budućnosti.

KLJUČNE REČI: pneumatik, model pneumatika, simulacija vozila

¹ *Pikula Boran, Faculty of Mechanical Engineering, University of Sarajevo, Vilsonovo šetalište 9 Sarajevo, Bosnia and Herzegovina, pikula@mef.unsa.ba*

Intentionally blank

CONTRIBUTION TO THE DEFINITION OF THE MOST IMPORTANT PARAMETERS FOR TIRE MODELS

Pikula Boran, PhD, associate professor, Trobradović Mirsad, MSc, assistant

UDC: 629.1;519.657

INTRODUCTION

Reliable prediction of vehicle motion using different simulation models is almost impossible without precisely defined forces at the contact of tire and road. Throughout the history, a large number of different models that describe the available adhesion between tire and road, and define the tire forces and moments has been developed. A useful brief overview of the different developed models is given in [3], [6]. The developed models, based on its approach, can be divided into several categories.

On one side, there are the experimental models, usually given in the form of tables or interpolation formulas (Pacejka „Magic formula“, Burckhardt). Given that they are developed on the basis of experimental results, these models show very good match with measured data. From the standpoint of time and computer resources they are suitable for use in vehicle dynamic simulation models. However, these models do not provide insight into the physical phenomena involved in the process of generating forces at the contact of tire and road. In addition, these models are valid only for specific tire in specific exploitation conditions. Changing any parameter causes a change in the final values of forces, that is changes the set of coefficients in the mathematical formulas.

On the other side, there are models based on physical assumptions and phenomena involved in the process of generating forces at the contact of tire and road. For a detailed analysis of the tire behavior complex models are used based on finite element methods. Due to the complexity and time needed for the calculation these models are not used within vehicle dynamics simulation models. For this purpose, more convenient are simple physical models (Brush, Dugoff, etc) that are easy on the budget, while allowing the physical understanding of tire behavior. These models show good match with experimental data, provided good definition of the values of influential parameters figured in equations (tire stiffness, friction coefficients, etc.), that change with a change of tire slip, vertical load, surface condition, etc. The aim of this study is to, based on analysis of experimental data sets, define the dependence of tire stiffness and adhesion coefficient as a function of the vertical load and the longitudinal and lateral tire slip.

EXPERIMENTAL DATA AND TIRE MODELING

The experimental data presented in [1] show the value of pure longitudinal force at the contact of tire and road during braking (Fig. 1), and pure lateral forces during cornering (Fig. 2). Results are given for dry asphalt surface.

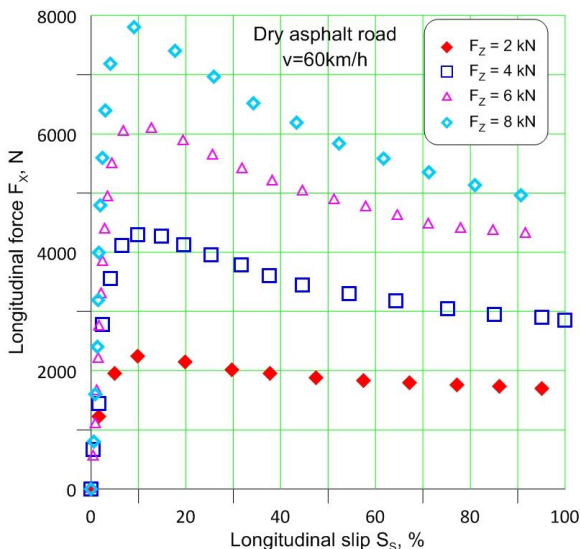


Figure 1 Experimental data for pure longitudinal force (pure braking), for different vertical loads [1]

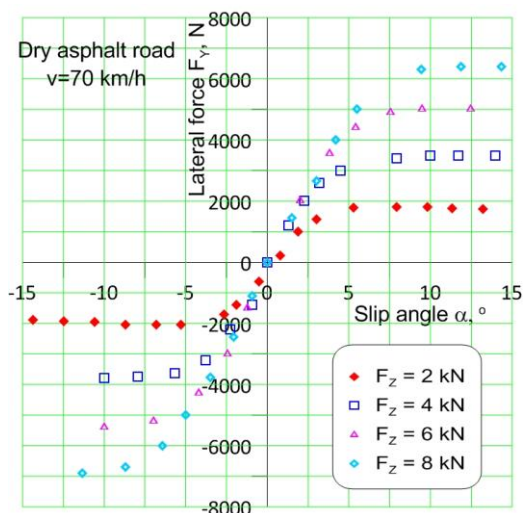


Figure 2 Experimental data for pure lateral force (pure cornering,) for different vertical loads [1]

By different models of adhesion, it is tried as accurately as possible to describe the available adhesion between tire and ground, i.e. to define the tire forces. Two simple physical models that have found extensive application in vehicle dynamics models are Dugoff model, and the Brush model.

Dugoff model [2], [3], [6], allows calculation of the tire longitudinal force F_x and tire lateral force F_y , assuming a uniform pressure distribution at the tire-road contact area.

$$F_x = C_s \frac{S_s}{1-S_s} f(\lambda) \quad (1)$$

$$F_y = C_\alpha \frac{\tan \alpha}{1-S_s} f(\lambda) \quad (2)$$

$$f(\lambda) = \begin{cases} (2-\lambda)\lambda, & \lambda < 1 \\ 1, & \lambda \geq 1 \end{cases} \quad (3)$$

$$\lambda = \frac{\mu F_z (1-\sigma_x)}{2\sqrt{(C_s S_s)^2 + (C_\alpha \tan \alpha)^2}} \quad (4)$$

where C_s and C_α are tire stiffness in longitudinal and lateral direction, S_s tire longitudinal slip, α tire slip angle, μ tire friction coefficient, F_z tire vertical load.

Longitudinal slip is calculated by the formula:

$$S_s = \frac{v_x - r_d \omega_w}{v_x} \quad (5)$$

where v_x is longitudinal wheel center velocity, ω_w wheel angular velocity, r_d wheel rolling radius.

More realistic, parabolic distribution of tire-road contact pressure is taken into account by the Brush model with parabolic distribution of contact pressure [4]. A Pacejka's interpretation of the Brush model with a parabolic distribution of contact pressure [3], [5] is shown below.

Longitudinal force F_x ,

$$0 < S_s < S_{sc}$$

$$F_x = 3\mu_x F_z \theta_x S_s \left[1 - |\theta_x S_s| + \frac{1}{3} (\theta_x S_s)^2 \right] \quad (6)$$

$$S_s < S_{sc}$$

$$F_x = \mu_x F_z \quad (7)$$

where S_{sc} is critical value of longitudinal slip at which complete tire began to slide, θ parameter which depends of tire stiffness, vertical load, and friction coefficient.

Value of tire slip S_s and S_{sc} , as well as parameter θ are calculated by the equations:

$$S_s = \frac{V_x - r_d \omega_w}{V_x}, \quad S_{sc} = \frac{1}{\theta_x} = \frac{3\mu F_z C_s}{C_s}, \quad \theta_x = \frac{C_s}{3\mu F_z} \quad (8)$$

Lateral force F_y ,

$$0 < S_\alpha < S_{\alpha c}$$

$$F_y = 3\mu_y F_z \theta_y S_\alpha \left[1 - |\theta_y S_\alpha| + \frac{1}{3} (\theta_y S_\alpha)^2 \right] \quad (9)$$

$$S_\alpha < S_{\alpha c}$$

$$F_y = \mu_y F_z \quad (10)$$

where is:

$$S_\alpha = \tan \alpha, \quad S_{\alpha c} = \frac{1}{\theta_y} = \frac{3\mu F_z C_\alpha}{C_\alpha}, \quad \theta_y = \frac{C_\alpha}{3\mu F_z} \quad (11)$$

One can see from the above models, the value of the available adhesion between tire and road, or tire forces are given in dependence of the longitudinal and lateral tire stiffness, friction coefficient between tire and road, and the tire vertical load.

Bellow, a brief analysis of the influence of aforementioned parameters on adhesion will be made, and the dependence of tire stiffness and adhesion coefficient as a function of the vertical load and the longitudinal and lateral tire slip will be defined.

ANALYZE OF INFLUENTIAL PARAMETERS

As mentioned above, as parameters influential to the process of generating forces at the contact of tire and road, in simplified physical models appear tire longitudinal and lateral stiffness, and friction coefficient between tire and road.

Tire stiffness

Tire longitudinal stiffness is defined as the slope of the curve of the longitudinal force at zero slip:

$$C_s = \left. \frac{dF_x}{dS} \right|_{S=0} \quad (12)$$

For experimental data presented in [1], tire longitudinal stiffness for different values of vertical loads can be calculated (Table 1).

Table 1 Tire longitudinal stiffness, for different vertical load – experimental data [1]

Vertical load F_z , N	Longitudinal stiffness C_s , N
2000	40000
4000	75000
6000	130000
8000	160000

Analyzing results, it can be noted that tire longitudinal stiffness changes linearly with the change of the tire vertical load (Figure 3).

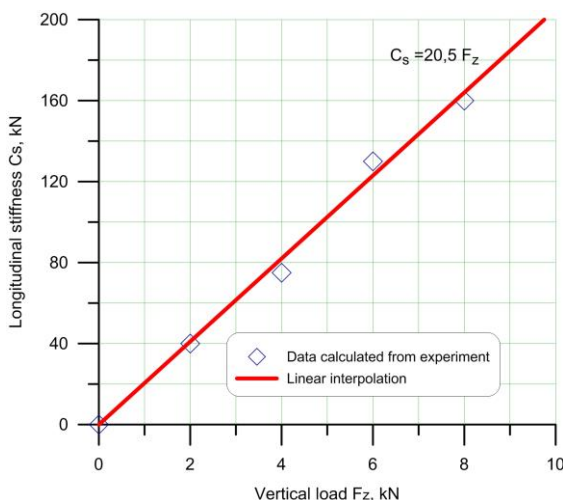


Figure 3 Tire longitudinal stiffness as function of vertical load

Adopting the assumption of linear dependence of the longitudinal stiffness of the tire vertical load, the relation can be established

$$C_s = K_1 F_z \tag{13}$$

where for the experimental results the coefficient $K_1 = 20,5$.

Tire lateral stiffness is defined as the slope of the curve of the lateral force at zero slip angle:

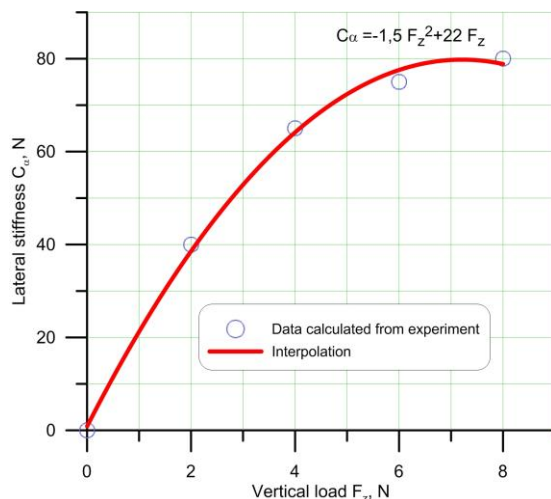
$$C_\alpha = \left. \frac{dF_y}{d\alpha} \right|_{\alpha=0} \tag{14}$$

For experimental data presented in [1], tire lateral stiffness for different values of vertical loads can be calculated (Table 2).

Table 2 Tire cornering stiffness, for different vertical load – experimental data [1]

Vertical load F_z , N	Cornering stiffness C_α N/°
2000	40000
4000	65000
6000	75000
8000	80000

Analyzing results, it can be noted that with the change of tire vertical load the tire lateral stiffness can be modeled as a parabolic function (Figure 4).

**Figure 4** Tire cornering stiffness as function of vertical load

Adopting the assumption of a square dependence of the lateral stiffness of tire vertical load, the relation can be established

$$C_\alpha = K_2 F_z^2 + K_3 F_z \quad (15)$$

Where for the given experimental results the coefficient $K_2 = -1,5$, and coefficient $K_3 = 22$.

Tire friction coefficient

Another influential parameter that figures in physical tire models is friction coefficient between tire and road. Using a study developed by Dugoff [2], and based on experimental results, it can be shown that friction coefficient is a function of slip velocity, and it can be presented in the following form:

$$\mu = \mu_0 (1 - M_1 v_s - M_2 v_s^2) \quad (16)$$

or

$$\mu = \mu_0 (1 - M_1^* S - M_2^* S^2) \quad (17)$$

where μ_0 is friction coefficient at zero slip, M_1 i M_2 reduced friction factors, v_s slip velocity, and S is tire slip.

Analyzing the influence of the vertical load on the longitudinal and lateral forces at the contact of tire and road, it can be seen that the friction coefficient changes with the tire vertical load. To take into account the influence of tire vertical load on friction coefficient a modification of the equation (17) for the friction coefficient is made, whereby linear effects of tire vertical load is assumed. Taking into account the mentioned, it can be established the following relation for friction coefficient:

$$\mu = C_1 S^2 + C_2 S + C_3 + C_4 F_z \tag{18}$$

where S is longitudinal slip S_x (for friction coefficient in longitudinal direction), or slip angle α (for friction coefficient in lateral direction), and C_1 to C_4 coefficients, and μ friction coefficient in longitudinal μ_x or lateral direction μ_y .

Analyzing experimental results for longitudinal force presented in [1], friction coefficient in longitudinal direction for different vertical load can be presented by equation (18), where the corresponding coefficients have values:

$$C_{1,x} = 3 \cdot 10^{-5}, C_{2,x} = -0,007, C_{3,x} = 1,27, C_{4,x} = -0,037$$

Experimentally determined and calculated values of friction coefficients in longitudinal direction are shown in the Figure 5.

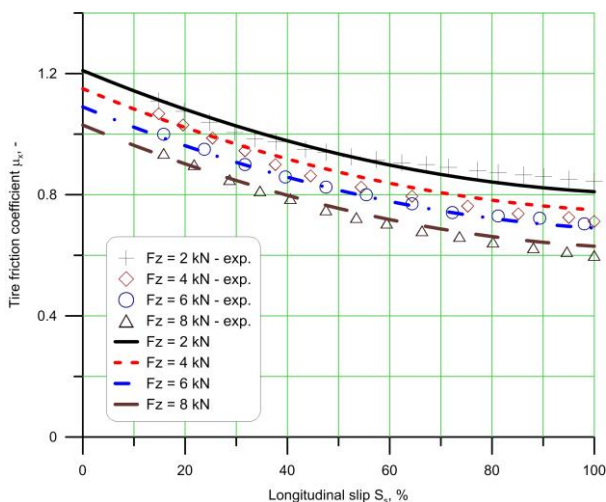


Figure 5 Longitudinal tire friction coefficient as function of vertical load and longitudinal slip - experimental data [1] and calculation

Analysis of the experimental results for lateral force presented in [1], shows that the friction coefficient in lateral direction for different vertical load can also be presented by equation (18), where corresponding coefficients have values:

$$C_{1,y} = -0,65 \cdot 10^{-3}, C_{2,y} = 0,017, C_{3,y} = 0,89, C_{4,y} = -0,029$$

Experimentally determined and calculated values of friction coefficients in lateral direction are shown in the Figure 6.

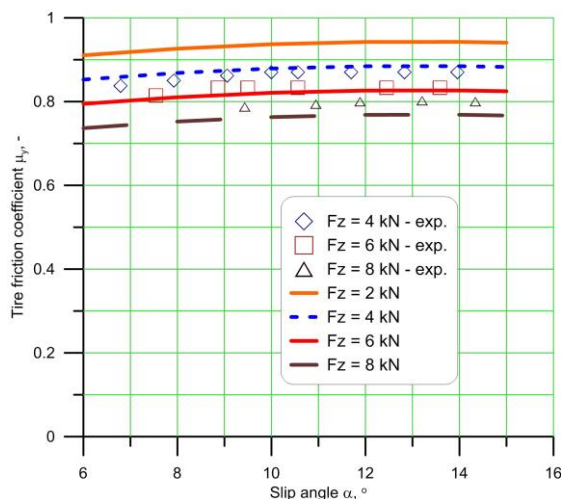


Figure 6 Lateral tire friction coefficient as function of vertical load and slip angle - experimental data [1] and calculation

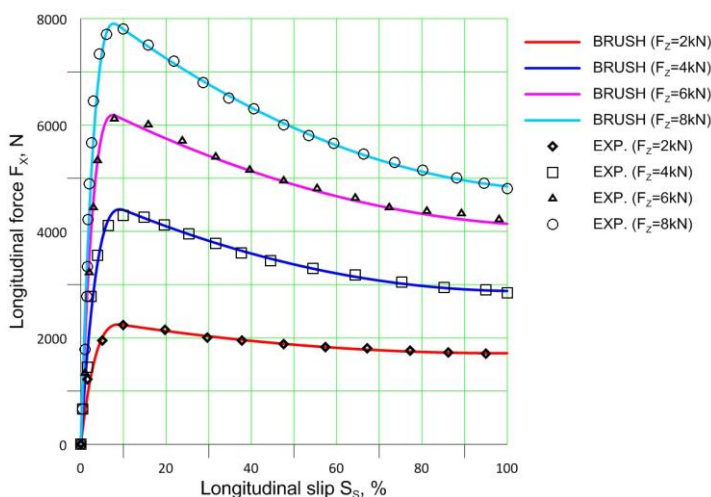


Figure 7 Tire longitudinal force – experimental data [1] and Brush model calculation

TIRE DATA CALCULATION

Entering values for longitudinal and lateral stiffness and friction coefficient of tire, based on experimental data from [1], in the equation for the Brush tire model, the values of longitudinal and lateral forces at contact of tire and road are obtained.

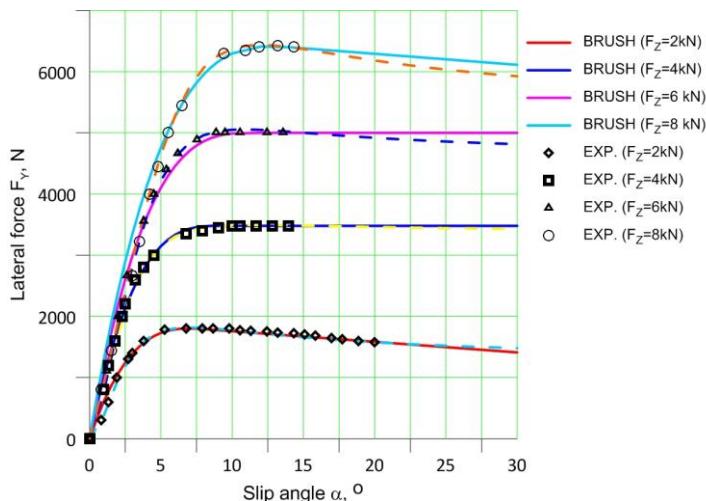


Figure 7 Tire lateral force – experimental data [1] and Brush model calculation

As seen on the above diagrams, for correctly determined values of stiffness and friction coefficient, Brush tire model shows exceptionally good match with the experimental results.

CONCLUSIONS

In the physical tire models, which are often used in vehicle dynamics simulations, tire stiffness and friction coefficient between tire and road are used as influential parameters. Correct choice of their values greatly affects the accuracy of those models and their applicability to vehicle dynamics simulation models.

Using experimental data available in literature, the paper analyzes the influence of tire slip and vertical load on the values of tire longitudinal and lateral stiffness, and friction coefficient. The influence of tire vertical load on the tire longitudinal and lateral stiffness is shown. The relations which show the dependence of the friction coefficient in function of tire slip are proven, and the assumptions about the effects of vertical load on friction coefficient in the longitudinal and lateral direction are given. For the available experimental data the equations and the corresponding coefficients are determined. By using this equation it is possible to calculate tire stiffness and friction coefficient, for different values of tire vertical load. For complete confirmation of obtained results further analysis of even greater number of experimental data is necessary.

With defined values of stiffness and friction coefficient, the calculation of tire longitudinal and lateral forces is carried out, using one of the physical tire models (Brush model with a parabolic distribution of contact pressure). The results show good match with experimental data. This way, it was shown that simple physical tire models provide quite satisfactory prediction of the tire forces values for the analysis of vehicle dynamics, but correctly determined values of stiffness and friction coefficient.

REFERENCES

- [1] Bakker, E., Nyborg, L., Pacejka, H. B.: "Tyre Modelling for Use in Vehicle Dynamics Studies", SAE Technical Paper 870421, Society of Automotive Engineers, Warrendale, PA, 1988
- [2] Dugoff H., Fancher P.S., Segel L.: "An Analysis of Tire Traction Properties and Their Influence on Vehicle Dynamics Performance", SAE paper 700377, 1970
- [3] Pacejka, H. B.: "Tyre and Vehicle Dynamics", Butterworth-Heinemann, Oxford, 2006
- [4] Pikula, B., Filipović, I., Trobradović, M.: "New Approach to Modelling of Adhesion Condition Between Tire and Road", 8th International Research/Expert Conference TMT 2004, Neum, BiH, 2004, page 471-474
- [5] Rajamani, R.: "Vehicle Dynamics and Control", Second Edition, Springer Science+Business Media, New York, 2012
- [6] Svendenius, J.: "Tire Modelling and Friction", PhD Thesis, Lund University, Sweden, 2007

EXPERIMENTAL BENCH FOR RECORDING IMAGES OF THE FLAME FRONT WHEN USING LASER PLUG IGNITION

Dejanu Marcel¹, Popa Dinel, Dascălu Traian, Tabacu Ion, Pârlac Sebastian

UDC:621.175

ABSTRACT: The experimental bench has in its composure a laser equipment, a high speed recording video equipment, a measuring system for recording pressure variations and a static enclosure in which experiments are conducted. The recording of images was done using the shadowgraph technique, a source of light with xenon and a 3000 frames/s high speed camera with a resolution of 512x512 pixels. There were recorded and analyzed the next phenomenon: the variation of the flame front depending on the initial pressure, the variation of the pressure from inside the chamber depending on the initial pressure and also the shape and the way of how the flame front is propagated. The results are presented under the form of images and diagrams.

KEYWORDS: bench, laser equipment, ignition, static enclosure, shadowgraph method.

EKSPERIMENTALNI MOST ZA SNIMANJE PLAMENOG FRONTA KORIŠĆENJEM LASERSKOG PALJENJA

REZIME: Eksperimentalni most opremljen laserskom tehnikom, za brzo snimanje, je merni sistem za snimanje varijacija pritiska i statičkog okruženja u kojem se odvija eksperiment. Slike su snimljene tehnikom senčenja: izvor svetlosti sa ksenonom i sa 3000 slika/s kamerom velike brzine rezolucije 512x512 pixels. Sniman je i analiziran naredni fenomen promene plamena zavisno od inicijalnog pritiska, varijacije pritiska unutar komore zavisno od inicijalnog pritiska i takođe oblik i način kako se plameni front prenosi. Rezultati su predstavljeni u obliku slika i dijagrama.

KLJUČNE REČI: most, laserska oprema, paljenje, statičko okruženje, metod senčenja.

¹ Received September 2012, Accepted November 2013

Intentionally blank

EXPERIMENTAL BENCH FOR RECORDING IMAGES OF THE FLAME FRONT WHEN USING LASER PLUG IGNITION

Dejanu Marcel¹, Popa Dinel, Dascălu Traian, Tabacu Ion, Pârlac Sebastian

UDC:621.175

INTRODUCTION

In the unfolding of the experimental research of laser ignition systems, several experimental solutions quoted by the specialty literature were taken into account that served as inspiration in constructing the experimental bench and having our own research methods. These were thought so that will correspond with the purpose we've set by using the financial and technological resources available. From all of these we've focused our attention on the experiments regarding the initiation of the burning process with methane-air or propane-air fuel mixtures.

In carrying out the experiments one prefers the methane-air mixtures. By choosing this type of fuel mixture one has several advantages like:

- The possibility of getting different concentrations easily,
- The ease of transportation,
- No auxiliary equipment needed to be introduced in the experimental burning chamber (like carburetion or injection equipments),
- The possibility of reaching high pressures in the combustion chamber without the use of any other equipment,
- The interest that the car producing industry has for the poorer methane-air mixtures in fueling internal combustion engines.

By using the methane-air mixture in fueling the spark ignition engines generates few inconveniences, mainly because of their specific chemical properties, specially the strong bond between C and H. These inconveniences are the delay in the fuel mixture ignition, misfires and premature failure of the spark plug. The spark plugs used for that purpose had to be replaced or cleaned every 500-700 hours of functioning at the most engines fuel with methane gas.

STATUS OF RELATED RESEARCH

From the articles published in this field of research, one will mention two in particular that are closer to its own experimental methods used in the laser induced ignition of methane-air mixtures:

- [1] "Laser spark ignition and combustion characteristics of methane-air mixtures", conducted by a team of researchers from the "Department of Electrical and Optical Engineering" from the University of Nebraska-Lincoln SUA, having as authors Jian X. Ma, Dennis R. Alexander and Dana E. Poulain.

¹ *Dejanu Marcel, Muntenia Invest S.A. Bucharest, Pitesti, Romania, dejanum@yahoo.com*

[2] "Fundamental of high-energy spark ignition with laser" conducted by a team of researchers from School of Mechanical Engineering of the University of Leeds UK, composed of: D. Bradley, C. G. W. Sheppard, I. M. Suardjaja and R. Woolley.

In the first case were conducted experiments regarding the propagation of the flame front in fuel mixtures of CH₄-synthetically air, for the case of classical ignition, compared with the laser induced ignition, all taking place in an experimental single cylinder. For initiating the ignition, the following types of lasers were used:

- Gas laser with Krypton Fluoride (KrF) that has a wavelength of $\lambda=248$ nm,
- Gas laser with Argon Fluoride (ArF) that has a wavelength of $\lambda=193$ nm,
- Solid laser with Neodymium and Al and Yttrium Garnet (Nd: YAG) that has a wavelength of $\lambda=1064$ nm.

One compared the initial ignition cores by analyzing the initial propagation phases of the fuel mixture. For the investigation an ultra-fast high-speed video camera was used. The burning initiation and radial expansion of the flame front were studied in different conditions of initial pressure and temperature specific to the real engine. The experiments proven that certain length laser beams generates radial expansion flame fronts that are ideal for the good functioning of the engine. The initial dimensions of burning cores and velocity of the flame front are calculated by using Raizer theory. Experiments proven that by using the laser beam to initiate the ignition, in the same conditions and same burning chamber, the time by which the pressure peak is achieved is reduced by 4 to 6 ms.

In the second case, the experiments were conducted in a burning chamber with 4 fans of variable speed, thing that facilitated the study of the flame front propagation in the case of passive and isotopic turbulences. The good viewing access allowed the researchers to record the plasma fronts propagation, the shock waves or the ignition cores with a high speed video camera in Schlieren method. A focalized beam from a laser with Nd: YAG initiated the electrical discomposure with beam energies of 85 to 200 mJ. The shock wave theory applied at the shock waves trajectory proves the necessity of high electrons energy, energy that is reached above 105 K and at high pressures. The values calculated for the absorption coefficient of the laser beam energy prove to be comparable with the one obtained experimentally. The propagation waves that results in the explosion creates mono circles in the flame front incensement areas. These generate a third lobe of the nucleus that is going to the laser focal core.

The displacement velocities of the laminar flame fronts are influenced by this dynamic-gas effect, by affecting the velocity of the flame, behavior not met in the classical ignition case. For poorer fuel mixtures that are close to the ignition limit, the strong dynamic-gas fluxes induced by the third lobe can collapse the flame front until extinction and can reduce the chances of laser induced ignition.

The third lobe disappears if the flame front becomes stabile as the initial dynamic-gas effects are repressed by the propagation of the flame front. This phenomenon was met also in the researches conducted by us as you will further.

RESEARCH METHODOLOGY

Stages of research

One established the next stages in the unfolding of the research:

Stage I - the preliminary testing of the fuel mixtures for determining the type of fuel that is most adequate for our research, also preparing and testing the experimental equipments for real usage.

Stage II - the advanced research of the ignition phenomenon that takes place in the static enclosure when initiating the ignition compared to the conventional spark plug or the laser pulse ignition generated by an external transmitter.

Stage III - constructing the laser plug based on the experimental data previously determined; testing the laser pulse ignition generated by the laser plug of the fuel mixture in the static chamber.

Full functional of experimental stand used during the research is presented in figure 1, where:

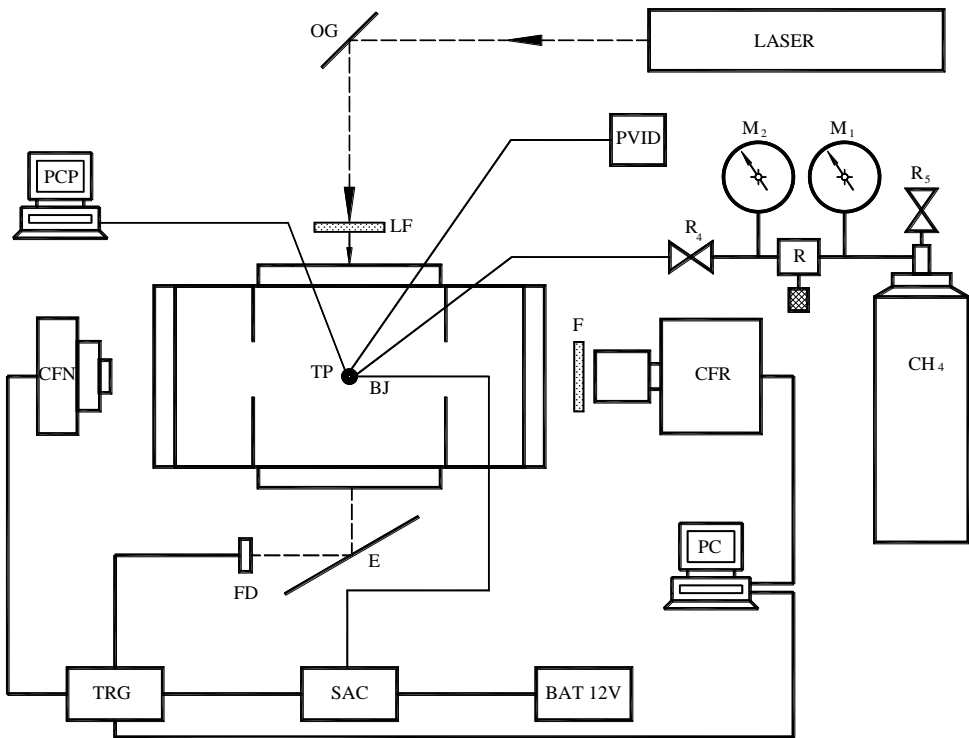


Figure 1 Functional diagram of experimental stand

- BAT 12V is a battery voltage of 12 V;
- SAC is the specific classical ignition engines Dacia type 810-99, of compound distributor type 3230 and induction coil type 3130;
- TRG is the trigger system;

- CFN is a video camera normal type of shooting digital Panasonic NV-GS 80 with a shooting speed of 50 frames/s;
- LASER is a laser transmitter type "Quanta Ray DCR, Nd-YAG 'with wavelength $\lambda = 1064 \text{ nm}$;
- LF is a plan lens focusing;
- GO is a laser ray redirection mirror;
- FD photodiode is the role of timing control system;
- E is the screen capture light signal;
- CFR is a camera with fast shooting speed type PHOTRON FAST CAM, which have captured images with a frequency of 1000 that 3000 frames / s;
- F is a filter protection to prevent the incidence of laser radiation with $\lambda = 1064 \text{ nm}$ directly on cameras video;
- PC is a computer with dedicated software for processing of images (CFR);
- TP is a transducer that senses pressure variations inside the static chamber and forward them to the system for measuring PCP;
- PCP is a device for measuring and recording pressure variations.

EXPERIMENTAL BENCH

Experiments in this stage were aimed at testing equipment under real conditions of operation, and achieve preliminary results that can be compared, analyzed between switching on the air-gas methane mixture with an electrical spark or with laser pulse.

The mixture fuel used was a mixture of synthetic gas, CH₄-air concentration of 12% (11.56%), bottled in a cylinder at 150 bar, equipped with a system for measuring the pressure of high and low, and with adjustable pressure regulator.

In figure 2, 3 and 4, is presented the experimental bench that is composed of: (1) –video camera shooting speed ; (2) – pressure transducer;(3) –the static chamber; (4) – optical window; (5) - normal video camera; (6) – high pressure manometer; (7) –optical window for viewing; (8) - photodiode; (9) – screen.

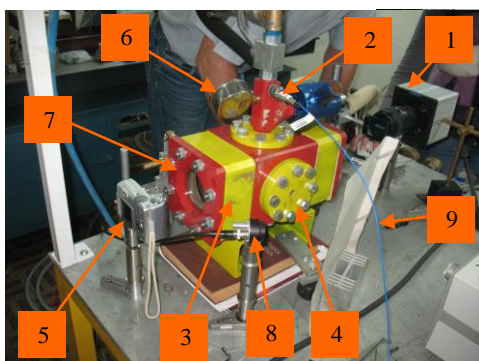


Figure 2 The experimental bench

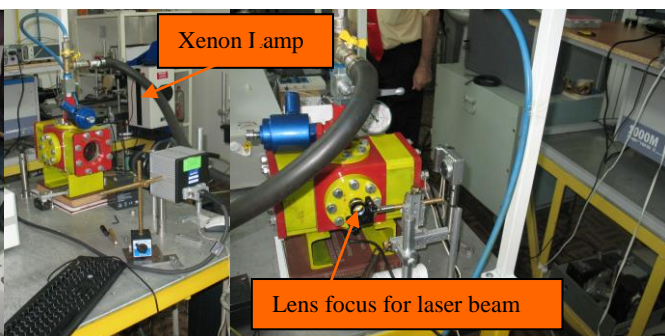


Figure 3 The experimental bench

Figure 4 The experimental bench

EXPERIMENTAL RESULTS ANALYSIS

In figure 5 are presented the photographs of the fuel mixture flame front propagation, for the electrical spark plug, comparative with laser pulse, transmitted by a fixed laser emitter in the following conditions: 12% methane-air fuel mixture, initial pressure of 0.1 MPa and the energy of the laser pulse of 22.8 mJ. In the case of classical spark ignition, as it can be seen, the flame front is easily obstructed in the inferior part by the electrodes compared to the laser induced ignition where the flame front can develop freely in the same are, because there is no obstacle in this case. In the same time, the flame front development is greater in the case of classical spark ignition for the same burning time. This can also be caused by the absence of the electrodes that causes turbulences.

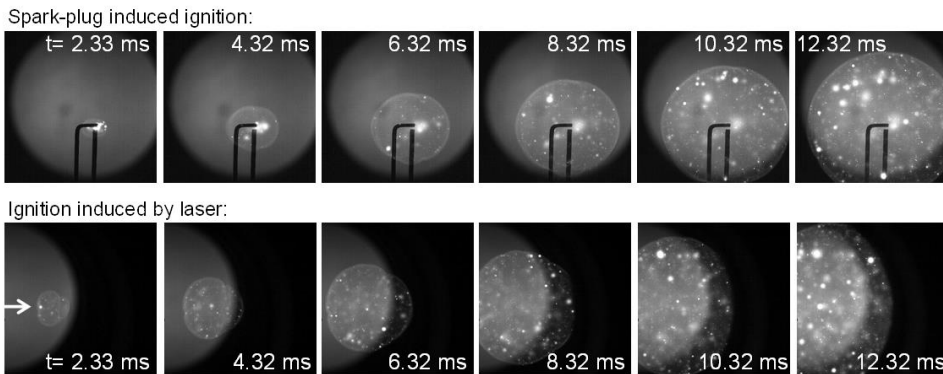


Figure 5 Photographs of the fuel mixture flame front propagation, for the electrical spark plug, comparative with laser pulse

In Figure 6, you can see the third lobe of flame front. Asymmetrical beam facilitates generation of plasma surface contour, and this behavior can inhibit development of the propagation of the flame.

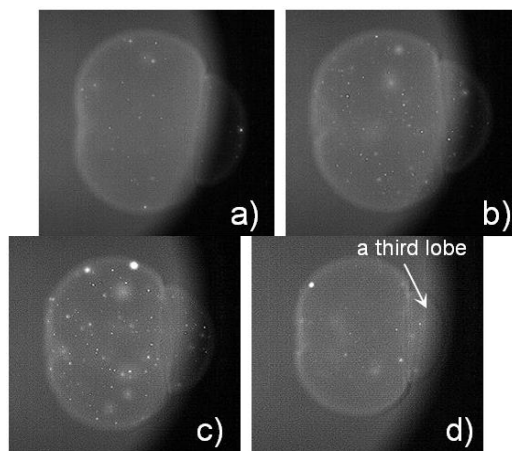


Figure 6 View the third lobe; initial pressure: a) 0.1 MPa; b) 0.2 MPa; c) 0.3 MPa; d) 0.5 MPa

Figure 7 presents the peak pressure variation in the explosion chamber of the methane-air fuel mixture ignition, for different values of the initial pressure, and the energy of the laser pulse of 22.8 mJ. For example, at an initial pressure of 0.101 MPa (1 atm), the peak pressure generated in the case of classical spark ignition was of 1.49 MPa and of 1.21 MPa in the case of laser induced ignition. At an initial pressure of 0.506 MPa (5 atm), the peak pressure raised to 3.66 MPa in the case of classical spark ignition and at 3.33 MPa in the case of laser induced ignition. These results could reveal that the presumption that the classical ignition could produce more energy than the laser ignition is false, even though the propagation in the second case was faster.

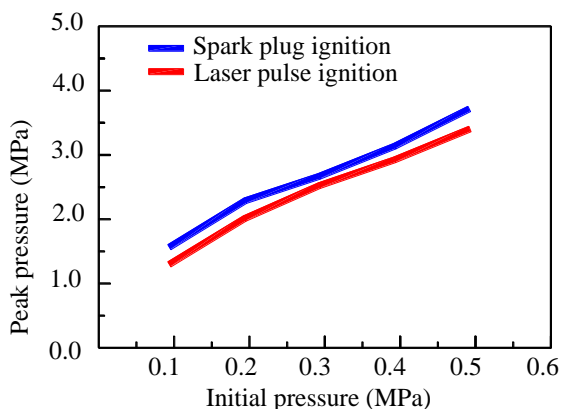


Figure 7 Peak pressure variation for different values of the initial pressure, and the energy of the laser pulse of 22.8 m.

In figure 8 is presented the time to the pressure developed by explosion increase from 10% of the peak value, to the maximum value of pressure, and the energy of the laser pulse of 22.8 mJ. Generally, the time to reach peak pressure is directly correlated with the initial pressure level. In the case of classical spark ignition the time to reach peak pressure raises from 23.3 ms, for an initial pressure of 0.101 MPa (1 atm.), to 28.7 ms for an initial pressure of 0.506 MPa (5 atm). The time to reach peak pressure is almost 10% higher in the case of laser induced ignition.

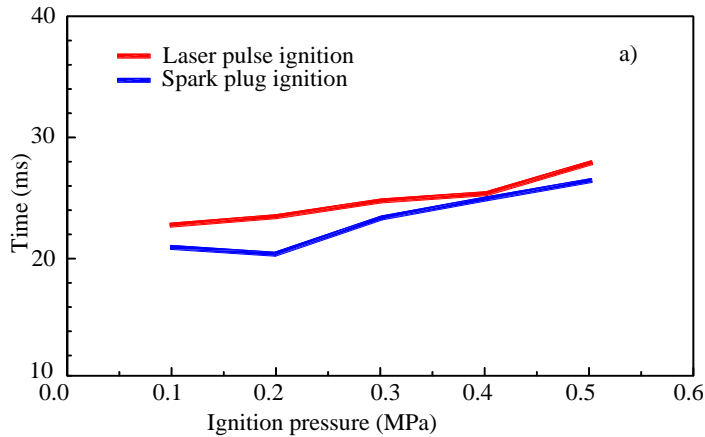


Figure 8 Time to explosion pressure increase from 10% of the peak value of the maximum value of pressure

In figure 9 are presented the variations of the flame front propagation velocity in the case of laser ignition and spark plug ignition, for different values of the initial pressures, pulse en and the energy of the laser pulse of 22.8 mJ. One can observe that the flame front propagation velocity is higher in the case of laser induced ignition, especially at high initial pressure. This behavior can be determined by the turbulent movements of the hot gas core generated by the plasma laser and by the influence of the spark plug electrodes over the flame front in the case of classical ignition.

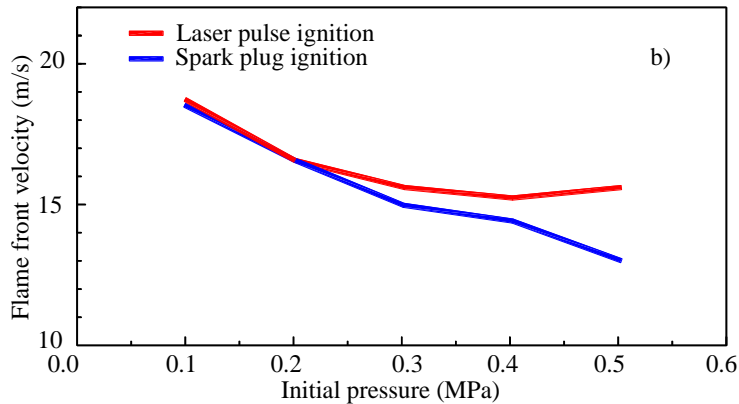


Figure 9 Variation of the flame front velocity depending on the initial pressure

In figure 10 are presented the variations of the flame front propagation velocity in the case of laser ignition and spark plug ignition, for different values of the initial pressures and for different value of energy pulse. One notices that a slight increase in the laser pulse energy conducts to a slight increase in the flame front displacement velocity. For example, for an initial pressure of 0.101 MPa (1 atm) the flame front velocity for a laser pulse energy level of 12.8 mJ, is of 16.4 m/s; the velocity increases at 18.4 m/s where the laser pulse energy reaches 22.8 mJ. Also one notates that the propagation velocity decreases once with the

increase in the initial pressure, so for a value of 0.507 MPa (5 atm) the propagation velocity drops to 15.4 m/s for a laser with the pulse energy of 22.8 mJ.

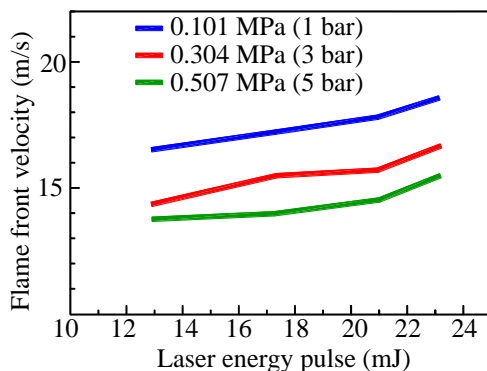


Figure 10 Variations of the flame front propagation velocity, for different values of the pulse energy and different initial pressures, laser ignition

CONCLUSIONS

The investigation of the preliminary phases of the burning process was done using the "shadowgraph" method, for capturing images of the flame front development from inside the chamber.

One concluded that the flame front generated by the laser induced ignition has the surface closest to the sphere and also has a much higher velocity than the one generated by the conventional spark plug; but the maximum pressure that was measured when using laser ignition, in the same initial condition, is slightly lower than the spark plug ignition.

The propagation velocity increases once with the increment of laser pulse energy and drops with the increment of the initial pressure in the combustion chamber.

REFERENCES

- [1] Beduneau, J.,L., Kim, B., Zimmer, L., Ikeda, Y., Measurements of minimum ignition energy in premixed laminar methane/air. Now by using laser induced spark, *Combust Flame*, 2003; 132:653–65.
- [2] T Bindhu, C.,V., Harilal, S.,S., Tillack, M.,S., Najmabadi, F., Gaeris, A.,C., Laser propagation and energy absorption by an argon spark, *Journal of Applied Physics* 2003;94(12):7402–7.
- [3] Bradley, D., Sheppard, C.G.W., Suardjaja, I.M., Woolley, R., Fundamental of high-energy spark ignition with laser, *Science direct, Combustion and Flame*, 138, pg. 55 – 77, 2004.Reference 4,
- [4] Dascalu, T., Dascalu, C., *Physics Of Lasers*, Editura Printech, 2006.
- [5] Dascalu, T., Pavel, N., High Temperature Operation of a Diode Pumped Passively Q Switched Nd:YAG/Cr4+:YAG Laser, *Laser Physics*, 2009, Vol. 19, No. 11, pp. 2090–2095.

- [6] Dascalu, T., Philips, G., and Weber, H., Investigation on Cr⁴⁺ passive Q-switch in CW pumped Nd:YAG LASER, *Optics & Laser Technology*, .vol.29, no.3, p.145 (1997).
- [7] Kofler a,H., Schwarz,E., Wintner, E.,Experimental development of a monolithic passively Q-switched diode-pumped Nd:YAG laser,) *Eur. Phys. J. D* 58, 209–218, 2010.
- [8] Kopecek, H., Wintner, E., Lackner, M., Winter, F., Hultqvist, A., Laser-simulated ignition in a homogeneous charge compression ignition engine. SAE 2004-01- 0937 2004.
- [9] Ma, J.,X., Alexander, D.,R., Poulain, D.,E., Laser spark ignition and combustion characteristics of methane–air mixtures, *Combust Flame* 1998;112:492–506.
- [10] McNeill, D.,H., Minimum ignition energy for laser spark ignition, *Proc. Combust. Inst.* 30 (2005) 2913–2920.
- [11] Salamu,G., Sandu,O., Voicu, F., Dejanu, M., Popa, D. Parlac, S., Dascalu,T., ș.a. Study of Flame Kernel Development in Methane-Air Mixtures Ignited by Laser. PACS, 42.55.-f; 42.60.-v; 47.70.Pq, *Novel Methods of Laser Technologies*.

RESEARCHES ON THE IMPACT OF HYPERMILING TECHNIQUES AND FUEL SAVING DEVICES IN ORDER TO REDUCE POLLUTION IN URBAN AREAS

Catalin Zaharia¹, Adrian Clenci

UDC:629.1.02

ABSTRACT: Techniques for super-economical driving are often known as hypermiling and very dedicated drivers can achieve astonishing economy through rigorous use of such techniques. Any method that contributes to the reduction of CO₂ emissions and which can be commercialised in a sensitive manner, must be applied to save the environment. Tests in both U.S. and Europe have shown ecodriving to reduce fuel consumption and emissions by up to 30%. In the meantime, European regulations set the emissions requirements for new vehicles at 130 g CO₂/km, with an additional 10 g CO₂/km to be achieved by additional complementary measures, including gear shift indicators. At this time there is little knowledge of how much fuel could be saved by the introduction of gear shift indicators, and there is no consensus on how these savings should be quantified.

Within this context, this paper presents a point of view on the need of on-board vehicle's indications for improving the driving style in order to reduce fuel consumption and pollutant emissions.

KEYWORDS: hypermiling techniques, driving style, pollutant emission, fuel economy

¹ *Received: September 2012, Accepted: September 2013.*

Intentionally blank

RESEARCHES ON THE IMPACT OF HYPERMILLING TECHNIQUES AND FUEL SAVING DEVICES IN ORDER TO REDUCE POLLUTION IN URBAN AREAS

Catalin Zaharia¹, Adrian Clenci

UDC: 629.1.02

INTRODUCTION

Green driving describes techniques that drivers can use to optimize their automobile fuel economy. The energy in fuel consumed in driving is lost in many ways, including engine inefficiency, aerodynamic drag, rolling friction, and kinetic energy lost to braking (and to a lesser extent regenerative braking). Driver behavior can influence all of these, (2). Since climate change and humanity responsibility has been widely accepted, many drivers have a new goal in mind: fuel efficiency. Eco-driving style is therefore often referred as smart driving because of the necessary complex tradeoff between the multiple goals the driver has to manage with.

Studies usually simplifies the green way to drive using simple advices easily understood by drivers (11), but sometimes leading to a misunderstanding of the fuel efficient driving strategy. Other studies used trial experiments before and after a training program to assess the eco-driving impact.

Effects of eco-driving on fuel consumption are well described in the literature, but results are often optimistic: CO₂ emissions reduction can be up to 30% according to many studies. The key question for policy makers is “how big” of an emission reduction we can get by encouraging an eco-driving style, taking into account the diversity in the way to learn eco-driving: just reading a few driving tips, taking a course with a professional, or doing practical exercises with equipped vehicles? Moreover, there is a need to understand the best way to teach and learn eco-driving style, especially for young drivers, (11).

ECODRIVING BASICS

Eco-driving primarily consists of a variety of driving techniques that save fuel and lower emissions.

Maintenance - key parameters to maintain are proper tire pressure and wheel alignment, and engine oil with low-kinematic viscosity referred to as low "weight" motor oil. Inflating tires to the maximum recommended air pressure means that less energy is required to move the vehicle. According to (10), under-inflated tires can increase rolling resistance by approximately 1.4 percent for every 1 psi drop in pressure of all four tires. Equally important is the scheduled maintenance of the engine (i.e. air filter, spark plug), and addressing any on-board diagnostics codes/malfunctions in the Engine Control Unit and related sensors, especially the oxygen sensor.

¹ *University of Pitesti, Automotive Dept., 1, Tg. din Vale, +40348453190, 110040, Romania, catalin.zaharia@upit.ro*

Efficient speeds and choice of gear (manual transmissions) - maintaining an efficient speed is an important factor in fuel efficiency. Optimal efficiency can be expected while cruising with no stops, at minimal throttle and with the transmission in the highest possible gear.

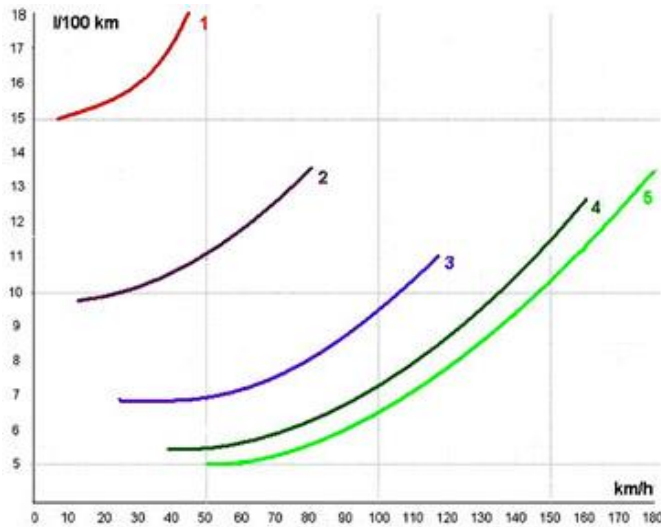


Figure 1 Fuel efficient driving, (12)

As seen in figure 1, 50 Km/h is best approached in 5th gear.

Engine efficiency varies with speed and torque, as can be seen in a plot of brake specific fuel consumption (bsfc). The graph contains also the isopower curves. For instance, 20 KW could be obtained in different ways: if using the highest possible gear imposing a low engine speed and a high engine load (e.g. 1500 rpm and 8 bar bmep, resulting from the intersection with the ideal green curve), then the bsfc will be about 265 g/KWh; at 3000 rpm and 4 bar bmep, i.e. with a lower gear, the bsfc increases at 330 g/KWh (figure 2).

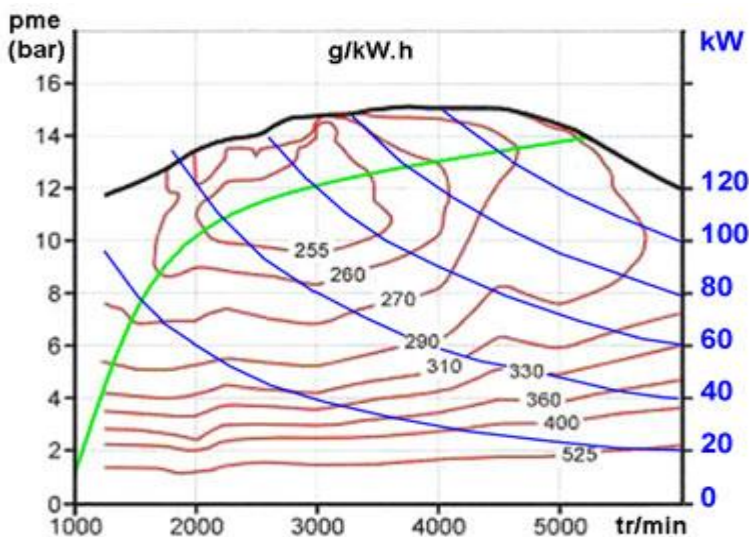


Figure 2 Brake specific fuel consumption, (12)

Anticipation - a driver may further improve economy by anticipating the movement of other traffic users. For example, a driver who stops quickly, or turns without signaling, reduces the options another driver has for maximizing his performance. By always giving road users as much information about their intentions as possible, a driver can help other road users reduce their fuel usage. Similarly, anticipation of road features such as traffic lights can reduce the need for excessive braking and acceleration.

Energy losses - understanding the distribution of energy losses in a vehicle can help drivers travel more efficiently. Most of the fuel energy loss occurs in the thermodynamic losses of the engine. The second largest loss is from idling, or when the engine is in "standby", which explains the large gains available from shutting off the engine.

Very little fuel energy actually reaches the axle. However, any mechanical energy that doesn't go to the axle is energy that doesn't have to be created by the engine, and thus reduces loss in the inefficiency of the engine. In this respect, the data for fuel energy wasted in braking, rolling resistance, and aerodynamic drag are all somewhat misleading, because they do not reflect all the energy that was wasted up to that point in the process of delivering energy to the wheels.

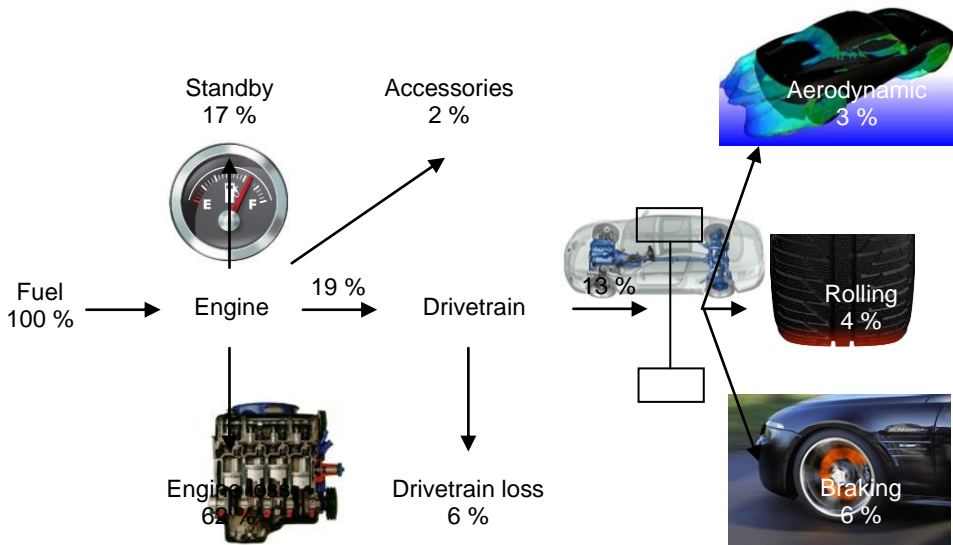


Figure 3 Energy flows for a late-model midsize passenger car – urban driving, (10)

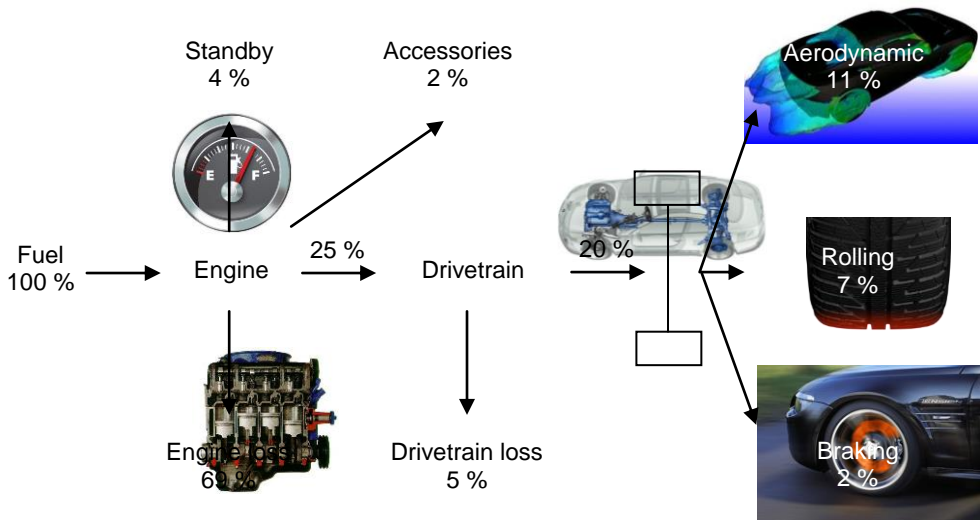


Figure 4 Energy flows for a late-model midsize passenger car – highway driving, (10)

The images (figure 3 and 4) report that on non-highway (urban) driving, 6% of the fuel's energy is dissipated in braking; however, by dividing this figure by the energy that actually reaches the axle (13%), one can find that 46% of the energy reaching the axle goes to the brakes. Also, additional energy can potentially be recovered when going down hills, which may not be reflected in these figures, (10).

Any statistic such as this must be based on averages of certain driving behaviors and/or protocols, which are known to vary widely, and these are precisely the behaviors which hypermilers leverage to the full extent possible.

ECODRIVING TOOLS

In order to meet the regulation regarding the reduction of fuel consumption, most of automobile manufacturers have generalised the solution of informing the driver about the moment of changing gear through the appearance on the instrument panel of certain icons under the form of arrows pointing to the inferior or superior plan, thus indicating to a higher/lower gear (figure 5), (1, 3). One may notice such systems came on the market with the introduction of the 6 gears box, the possibilities of approaching the driving being increased.



Figure 5 Gear change indicator – Audi A4 B8

In what follows, some more complex solutions adopted by certain automotive manufacturers will be presented.

Honda's Ecological Drive Assist System - EcoAssistTM – represents a feedback system for the driver, accomplished with the purpose of contributing to the developing and maintaining of a driving style that is more efficient from the point of view of fuel consumption, (6, 7). The system monitors the driving style and can display its impact on the fuel economy of the automobile. The driver can then make adjustments in the style of driving in order to maximize fuel economy.

Nissan Motor Co, Ltd., launched the ECO accelerator pedal – the first technology of this kind in the world, designed to help drivers diminish fuel consumption (figure 6). When the ecological pedal system is turned on, each time the driver presses the accelerator, he/she activates a mechanism that registers fuel consumption. In case the system detects an excessive pressure, the ECO pedal pushes back the driver's leg, thus sending the information that he/she is using more fuel than necessary. An ecological consumption indicator integrated in the instrument panel provides in real time the driver with the levels of energetic consumption, thus helping him/her improve the driving conditions. The ECO pedal system can be activated or deactivated, function of the driver's preference. Nissan has commercialised automobiles that are equipped with ECO pedal since 2009. The research done by Nissan showed that, by using ECO pedal system, the drivers can diminish their energetic consumption by 5-10%, function of the driving conditions, (9).

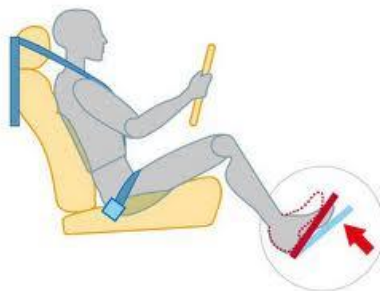


Figure 6 Eco accelerator pedal – Nissan

Software and hardware based

DriveGain Ltd. – DriveGain App., (10) The DriveGain App uses the iPhone's built-in GPS system to calculate the vehicle's speed and rate of acceleration and deceleration. The visual displays include a recommended gear indicator and some sliders that drivers try to keep in the green. In addition, the App calculates fuel consumption, CO₂ emissions and fuel cost per mile. By following the on-screen cues, DriveGain claims that it can help users save money on fuel while reducing CO₂ emissions by up to 660 kilograms per year. The App's database has over 16,900 different vehicles to choose from, however hybrid vehicles are not yet supported.

Garmin Ltd.: ecoRoute, (10). With the ecoRoute software on the GPS systems, drivers can save money on fuel costs by finding more fuel-efficient routes. These routes are selected by factoring in fuel consumption data, the number of stops and speed limits, as well as further traffic circumstances. ecoRoute also gives a real-time feedback on the efficiency of the way of driving. ecoRoute's Fuel Report automatically calculates details about the travel time and fuel usage. The Drivers can see time and distance traveled as well as the cost of fuel used

and average fuel economy. The ecoRoute Driving Challenge makes a game out of saving gas by keeping a running score that reflects the current driving habits.

PH Informática – EcoSpeed, (10). EcoSpeed is an iPhone App that is available for free at the Apple App Store. The speedometer uses the gearbox settings and GPS data to help the Car Owners to drive more efficiently and save money. It also presents useful information while driving. Features of the app are: gear adviser, speedometer, top speed alert, sound alerts, GPS position, GPS signal.

Quality Alliance Eco-Drive – App., (10). By capturing refueling behavior and tire pressure settings, users of this iPhone App receive information about fuel consumption, saving potentials with ideal tire pressure, price development of fuel and the CO₂ emissions. The app can be downloaded for free.

Toyota Motor Marketing Europe – A Glass of Water, (10). The iPhone App – "A Glass of Water" mimics a glass of water placed on a car's dashboard and challenges users to not spill a drop. Toyota estimates that the gentler driving style encouraged by this App would help consumers lower their fuel consumption by 10 percent, resulting in the lowering of CO₂ emissions by 2 million tons a year. The App reacts to the driving behavior as if the driver had an actual glass of water on his dashboard: accelerating too fast or braking too suddenly will spill water. It also records the driving distance, time, fuel consumption and water spilled. After each drive the users can analyze their results and see on a map where they can improve their driving for the future. The results are automatically uploaded to the "A Glass of Water"-Website and compared to other participants.

Volkswagen AG; MTV Networks – CO₂ monitor, (10). By interviewing over 26,000 young people worldwide, Volkswagen and MTV Networks compiled the "MePublic" social media study. The international study gives an insight into media use and value concepts among the group of 14- to 29-year-olds known as "digital natives". As the study shows, the young people would also like to see networking extend to the car. With the help of the iPhone App "CO₂ monitor", fuel consumption and other driving data is transmitted to a Volkswagen website and included into a driver ranking. Volkswagen is seeking to motivate its customers to develop an awareness of environmentally-friendly and fuel-efficient driving with this edutainment competition.

KIA Motors Corp. – Eco Driving System, (10). The KIA Eco Driving System consists of an eco-lamp on the dashboard, which will guide the driver to drive in the most economical way. A green lamp will come on to indicate high fuel efficiency driving (i.e. traveling at a constant speed), while a red lamp will indicate low fuel efficiency (i.e. sharp acceleration, sudden braking). A white lamp will come on to show normal fuel efficiency or standby mode. The system is designed to encourage eco-driving by providing real-time feedback to the driver.

Nissan Motor Co. Ltd. – Eco-Drive and You, (10). Nissan is adding a new service called "Eco-Drive and You" for its on-board CARWINGS navigation system in Japan. Since January 2007, Nissan CARWINGS members have been provided a range of services that have included fuel-efficiency rankings among owners of the same model and advice on efficient driving methods. The service has now been expanded to provide the same content found online via the onboard navigation system of car owners. Car owners can monitor their

fuel consumption habits, experience better fuel-economy as well as receive helpful driving tips while on the road. The service has three main components:

- ecodrive check (audio and video display). This displays average fuel consumption, fuel consumption trends and the fuel consumption history and comparison to the last two records.
- ecodrive ranking (audio and video display). This displays average fuel consumption history, the driver's ranking among CARWINGS members with the same model and fuel expense annual savings.
- driving advice (audio guidance). This covers various topics for the driver, which also includes tips on better fuel efficiency.

Toyota Motor Corporation – Eco Drive Indicator, (10). Based on a comprehensive determination that takes into consideration factors such as accelerator use, engine and transmission efficiency and speed and rate of acceleration, the Eco Drive Indicator, located on the instrument panel, lights up when the vehicle is being operated in a fuel-efficient manner. This is supposed to raise the driver's awareness towards environmentally considerate driving and contribute to fuel economy. Although results may vary – depending on the level of traffic and conditions such as the frequency of starts from stop and of acceleration, as well as distance driven – the Eco Drive Indicator can improve fuel efficiency by approximately 4 % (as measured by Toyota).

Fiat Group Automobiles Germany AG: eco:Drive, (10). eco:Drive was launched in October 2008 as a software application that is free to download at Fiat's website. It works by asking drivers to plug a USB stick into their Blue&Me infotainment system (presented in all new Fiat models), where it records telemetric data from the car's network. Plugging the USB into a computer allows the Fiat servers to analyze the journey data, on an anonymous basis. Algorithms measure driving efficiency based on four parameters: steady acceleration, steady deceleration, early gear changes and moderate and consistent speed. Drivers receive a star rating (out of five) for each of these indicators, and their performance overall on the four indicators is used to calculate an eco:Index score out of 100 – a higher score means more efficient driving. Drivers receive tailored advice on how to improve their performance on each indicator, and thus their overall eco:Index. Through their computer, they can track improvements over time, set targets and see how much CO₂ they are saving. "ecoVille" – an online community which shows the latest number of drivers using eco:Drive and the total CO₂ emissions that eco:Drivers have saved up to date, has also been developed in connection to the application (figure 7).



Figure 7 Ecodrive - Fiat

Ford Motor Company: Econo Check, (10). The Ford Econo Check App calculates potential fuel savings for any car - based on make, model, age and annual mileage - and picks up fuel efficient driving tips on any iPhone or iPad. Ford Econo Check enables Ford vehicles to be

fitted with a data logger to monitor how they are driven. Once the Econo Check chip is removed and data downloaded, a tailored report advises how modifying gear changes, anticipation, acceleration and braking will improve fuel economy. Resulting savings are also shown, which can be up to 25 % a year according to a study of 50,000 drivers.

PLX Devices Inc.: Kiwi, (10). The Kiwi is a plug and play device compatible with all 1996 vehicles and up. Kiwi plugs into the existing on board diagnostic port (OBDII), located near the steering column. From this port, Kiwi is able to obtain detailed sensor information about the vehicle. A multitude of sensor data including vehicle speed, RPM, engine load, oxygen sensor readings are all analyzed to determine the vehicle's optimum driving efficiency. The PLX Kiwi uses mathematical algorithms to analyze the engine's performance and driving behavior. The drive green lessons are designed to improve smoothness, drag, acceleration, and deceleration parameters. The Kiwi software operates much like a game. While driving, the daily goal is to obtain the highest "Kiwi Score" possible through an ecodriving style.

FES GmbH – ECOdrive III, (10). Connected to the control unit of passenger cars, transporters or trucks, the ECOdrive III allows its user to regulate the engine speed and maximum speed of the vehicle. The maximal engine speed depends on the charge and loading of the vehicle. If the vehicle has to drive uphill or with a higher loading the system allows a higher engine speed to always guarantee the adjusted maximum speed.

SR-Car Expert e.K. – Eco Tuning, (10). SR-Car Expert's Eco Tuning leads to a reduction of fuel consumption by changing the motor software of the vehicle. The remaining durability of the vehicle and an additional reduction of CO₂ emissions are further features of the Eco Tuning software. During several test rides, the tuning could lead to an average reduction of the fuel consumption by 15-20 %.

OFF-BOARD METHOD TO EVALUATE THE DRIVER BEHAVIOR

Prior to use a car, people may be trained in ecological & economical Driving (Eco²Driving) by using a driving simulator. Because the training journeys are not made in a real vehicle, fuel can also be saved. In addition, there is no need for a test track. Important facts (5, 8):

- eco²drivers use 10 to 15 per cent less fuel than people without course experience – even at a slightly higher average speed.
- eco²driving influences positively the ride comfort and vehicle wear and tear. Eco²drivers achieved significantly better measurable values than persons without course experience.
- eco²drivers remain eco²drivers.
- theoretical knowledge of basic eco²driving rules alone is insufficient. Practical experience is essential to master the technique: a clear indication of the benefits of eco²driving training.

Car simulators are used in various research areas: evaluation of driver's behavior, their education and training, testing and implementing new systems, research on the dynamics of wheeled vehicles, traffic safety studies.

To use a car simulator in research and education the virtual reality system must reproduce the vehicle dynamics and its interaction with the environment in a most realistic manner. It is well known in the specific literature that a car simulator cannot reproduce 100% real life situations or sensations and accelerations experienced by the driver because of reduced space working and limitations actuators.

Car simulators reproduce the vehicle dynamics and its interaction with the environment (traffic signs, buildings, other vehicles, etc., figure 8). This kind of simulation was used for the first time on the fly simulator.



Figure 8 *Driving simulators*
(CARRS – Q: Center for Accident Research and Road Safety)

Applying this concept in the automotive industry, generated a wide interest, Volkswagen built the first such simulator in 1970. Over the past 40 years, car simulators have become research tools used with confidence in different applications.

Different systems are tested to study their performance and limitations before being implemented in an expensive prototype vehicle. Therefore, different studies are performed using a simulator under conditions which would not be safe to be performed in the real world.

A topic of great interest in the automotive industry is the development and implementation of advanced driving assistance (ADAS). Testing these systems together with the study of acceptance by the user is essential before implementation in mass production.

Car simulators cannot play in an identical mode vehicle accelerations that it simulates, regardless of available workspace and the number of degrees of mobility.

Therefore, different strategies are used in order to achieve a realistic virtual environment, for example: development of intelligent control algorithms, the use of a visual field of 360⁰, simulation of vehicle noise, etc. Nevertheless, the use of these systems presents different disadvantages: validation of results, limited workspace, mistyped simulation components and that can cause discomfort to the user.

CONCLUSIONS AND FUTURE WORKS

This study will contribute at developing a simulation model of automobile functioning with the goal of realising a graphical interface that will assist the driver in real time for the adoption of a driving style with minimal influence on fuel consumption, implicitly on CO₂ emissions.

The study will establish a set of rules that meet the needs of automobile users with the primary purpose of adopting an eco²driving. This set of rules will be implemented in the activity of University of Pitesti driving school STUDENT AUTO.



Figure 9 Driving school STUDENT AUTO – University of Pitesti, Romania

Therefore, the authors will use techniques of semiempirical modelling of internal combustion engine and equipping the automobile with specific devices and testing it with various drivers on a predefined urban route (the city of Pitesti). These tests will contribute to the establishing of the particularities related to the driving styles observed. For the simulation, the authors will take advantage of the possibilities offered by the CRUISE software, provided by the AVL List Austria, to whom many thanks are addressed.

REFERENCES

- [1] Barth, M., Kanok Boriboonsomsin, “Energy and emissions impacts of a freeway-based dynamic eco-driving system”, ScienceDirect, Journal of Transportation Research Part D 14 (2009) 400–410
- [2] Barkenbus, Jack N. “Eco - driving: An overlooked climate change initiative”, ScienceDirect, Journal of Energy Policy 38 (2010) 762–769
- [3] Beckx C., L. Int Panis, I. De Vlieger & G. Wets, “Influence of gear – changing behaviour on fuel use and vehicular exhaust emissions”, Proc. 8th Highway and Urban Environment Symp. – In Highway an Urban Environment, Springer, Netherlands, p. 45 – 51, 2007.
- [4] Beusen, B., Steven Broekx, Tobias Denys, Carolien Beckx, Bart Degraeuwe, Maarten Gijbsers, Kristof Scheepers, Leen Govaerts, Rudi Torfs, Luc Int Panis, “Using on-board logging devices to study the longer-term impact of an eco-driving course”, ScienceDirect, Journal of Transportation Research Part D 14 (2009) 514–520.
- [5] Cumpelik, J., “ECODRIVE – driver training”, Conferinta ECODRIVEN - EEBV, Prague, novembre 2008
- [6] C.J.G. van Driel, F. Tillema, Dr. M.C. van der Voort “Directives for new-generation Fuel Economy Devices”, CE&M research report 2002R-004 / VVR003 ISSN 1568-4652
- [7] De Vlieger I., D. De Keukeleere & J. G. Kretschmar, “Environmental effects of driving behaviour and congestion related to passenger cars”, Proc. Int. Symp. Transport and Air Pollution, Graz, Austria, 31 may 1999, Atm. Env., vol. 34, no. 27, p. 4649 – 4655
- [8] Hennig, W., “Best practice training & evaluation. Improving fuel economy, reducing CO₂”, Conferinta ECODRIVEN - EEBV, Prague, November, 2008.
- [9] Orofino, L., “EcoDrive: Driver behaviour evaluation system to reduce CO₂ emissions”, FISITA 2010, F2010E052, may – june 2010, Budapest, Hungary,
- [10] www.wikipedia.fr, “Fuel economy – maximizing behaviors”,
- [11] www.cieca.be, “Driving training and driving tests”,
- [12] www.auto-innovations.com, “Comment consommateur moins”

MODELLING VALVE DYNAMICS AND FLOW IN RECIPROCATING COMPRESSORS

Dr Dobrivoje Ninković, doc. dr Dragan Taranović, mr Saša Milojević¹, PhD Candidate and dr Radivoje Pešić, Full Professor, University of Kragujevac, Faculty of Engineering

UDC:629.3.018.2

Summary

Thermodynamic performance (delivery rate and power intake) and reliability of reciprocating compressors are dependent upon the valves. Since the valves open and close automatically, there is a high degree of coupling between the gas flow through the valve and the sealing element dynamics; a mismatch between the two leads inevitably to degradation of the compressor performance and/or short valve life. The latter is due to impact forces between the sealing element and other parts of the valve assembly. Therefore, matching the valves to the compressor application at hand is a complex task that calls for the use of the corresponding simulation models.

Surveyed in the paper are mathematical models for the prediction of the valve performance, consisting of the sub models describing compressible gas flow through the valves, sealing element dynamics, and the interaction of the latter with the flow. Flow models based on the discharge coefficient are intrinsically not able to predict the critical flow regime with sufficient accuracy, requiring thus experimental data that are not always available. It is also suggested that other loss calculation approaches, such as the stagnation pressure loss model, should be investigated as possible alternatives to the discharge coefficient concept.

Key words: Valve dynamics, Valve flow, Discharge coefficient, Reciprocating compressor.

MODELIRANJE DINAMIKE VENTILA I PROTOKA U KLIPNIM KOMPRESORIMA

UDC:

Rezime

Termodinamičke performanse (isporuka i usisna snaga), i pouzdanost klipnih kompresora zavise od funkcionalnosti ventila. Obzirom da se ventili otvaraju i zatvaraju automatski, njihov protok zavisi od dinamike ventila; njihove neusaglašenosti dovode do pogoršanja performansi kompresora i/ili kraćeg veka ventila. Tome doprinose udarne sile između zaptivnog elementa i delova ventila. Prema tome, izbor kompresorskog ventila je veoma složeno pitanje i zahteva primenu odgovarajućih simulacionih modela.

U radu je dat pregled matematičkih modela za proračun performansi ventila, u okviru kojih su integrisani submodeli za opisivanje protoka stišljivog gasa kroz ventil, dinamiku zaptivnog elementa i njegovu interakciju sa protokom. Modeli protoka bazirani na određivanju koeficijenta isticanja su neodgovarajući za preciznije određivanje kritičnih režima protoka, gde se zahtevaju eksperimentalni podaci koji nisu raspoloživi. Predloženo je da se proračun ostalih gubitaka određuje modelom gubitaka usled pada pritiska, kao moguća alternativa koncepciji određivanja koeficijenta isticanja.

Ključne reči: Dinamika ventila, protok ventila, koeficijent isticanja klipni kompresor.

¹ Saša Milojević, PhD Candidate, University of Kragujevac, Faculty of Engineering, www.fink.rs, E-mail: tiv@kg.ac.rs

Intentionally blank

MODELLING VALVE DYNAMICS AND FLOW IN RECIPROCATING COMPRESSORS

Dr Dobrivoje Ninković, doc. dr Dragan Taranović, mr Saša Milojević¹, PhD Candidate and dr Radivoje Pešić, Full Professor, University of Kragujevac, Faculty of Engineering

UDC: 629.3.018.2

1. INTRODUCTION

Reciprocating compressors are widely employed in a number of industry and transportation branches, and it can be freely stated that some of the applications would hardly be possible without this type of machinery. The latter refers to such extreme cases as compressing ethylene to pressures upwards of 300 MPa for the purpose of producing LDPE (low-density polyethylene), very low suction temperatures (of the order of -150 °C) in the field of liquefied gas transport and storage, or for compressing gases contaminated with particles. In commercial vehicles for road transportation, reciprocating compressors are customarily used for obtaining pressurized air for auxiliary purposes, such as braking, gear shifting, etc. Common to almost all reciprocating compressor applications is the fact that the compressor is a rather small component in comparison with the process and/or system that it supplies with gas, but its reliability determines the availability and safety of the entire plant. Therefore, the plant designers and owners require trouble-free operation from their compressors over long periods of time. Indeed, expected service time for a small hermetic compressor in a common household refrigerator is more than 20 years.

Conceptually, a reciprocating compressor stage consists of a cylinder, the volume of which varies periodically due to the motion of a piston that closes one end of the cylinder. The other end of the latter is closed by two valve sets, one each for admitting the gas to be compressed into the machine (suction valve), and for allowing the high pressure gas to be delivered to the process and/or machines utilizing it (discharge valve). One speaks here in terms of valve sets because there are machines (usually large process compressors) which may be equipped with more than one valve pro suction and discharge side, respectively.

From the standpoint of thermodynamic performance, the cylinder must be completely sealed at both ends during the compression process, and the suction and discharge processes are to be realized exclusively through the respective valves, which translates into the zero-leakage requirement for the machine. While the piston can be reliably sealed by means of one or more rings (lubricated or dry-running) that press against the cylinder wall, securing zero-leakage function of the valves is by no means a simple task.

The key feature of compressor valves that simultaneously affects both their sealing performance and reliability is that they, unlike their counterparts in a conceptually similar IC engine, are not actuated. They are held closed by elastic forces internal or external to the sealing element; and they open and close automatically, in accordance with the balance of gas pressure forces and the previously mentioned elastic ones. Under the gas pressure forces one understands both the force due to static pressure difference across a closed valve and the

¹ *Saša Milojević, PhD Candidate, University of Kragujevac, Faculty of Engineering, www.fink.rs, E-mail: tiv@kg.ac.rs*

aerodynamic drag brought about by the gas flow impinging onto the sealing element in a partially or fully open valve. Clearly, a high degree of coupling between the gas flow and the sealing element motion, nowadays referred to as fluid-structure interaction (FSI), is to be expected in such a device. The latter and the absence of a reliable guide device that would provide for the plan-parallel motion of the sealing element give rise to non-parallel impacts between the latter and other parts of the valve assembly, leading to the so-called Dynamic Stress Concentration Effect [6], which in turn causes premature sealing element fracture and the machine shutdown.

According to a survey carried out in the process compressor field in 1996, compressor valves represent the primary cause of unscheduled reciprocating compressor shutdowns, with a relative frequency of 36% [23]. Since the second-ranking cause of machine failure is piston rod packing (17.8%), which are present only in crosshead and compound machines, one may surmise that valves are responsible for even a larger percentage of failures in small compressors, such as e.g. used to compress air in commercial motor vehicles.

Given the passive nature of the automatic compressor valves, the mass-spring oscillatory system of the sealing element cannot be fully matched to the compressor over a wide range of operating conditions. While large process compressors normally run either at a constant speed or within not very wide speed ranges, giving thus the valve designer a chance to optimise the valve parameters or even excludes dangerous compressor speeds, this is definitely not the case with small air compressors of commercial vehicles. The latter is expected to perform reliably within the entire engine speed range, i.e. from the idle to the maximum rpm. The matching and optimisation of the valves have been the subject of active research in the past several decades, resulting in a body of knowledge whose salient features are to be surveyed in the present contribution.

2. VALVE MODELLING

2.1. GENERAL CONSIDERATIONS

Conceptually, the influence of the valve upon the compressor performance and reliability can be analysed in terms of the following three phenomena, i.e. models:

1. Mechanical, accounting for the opening and closing processes motion of the spring-mass assembly of the sealing element, and whatever impact processes within the valve. This area is commonly referred to as valve dynamics.
2. Flow, describing the relationships between the mass flow rate through the valve and the gas states in the cylinder and the valve attachments.
3. Coupling i.e. interaction between the valve action and the fluid dynamics at the upstream and downstream sides of the valve.

While the first two phenomena can be studied both analytically and experimentally in isolation from the compressor i.e. by specifying constant or variable fluid states upstream and downstream of the valve, the third one is a system phenomenon and can thus only be analysed together with the cylinder and the attached piping and fittings. Experimentally, the latter calls for measurements at a suitable test rig or in the compressor installation; and analytically, a comprehensive system model is needed that includes all relevant components and processes. Regarding the modelling depth, it was an established practice in the past to lump the respective piping at the suction and discharge sides of the machine into volumes, neglecting thus the wave motion that inherently takes place there. This approach simplifies

the plant model considerably, saving also the computation time. MacLaren [30] argued that the accuracy of performance prediction is affected by this simplification, and it was shown in [13][32][33][21] that large differences do exist between the performance figures obtained with the two model assumptions. However, further discussion of this subject is beyond the scope of the present paper.

2.2. MODELLING OF THE VALVE DYNAMICS

In principle, an automatic compressor valve consists of a movable sealing element, a seat against which the latter rests when the valve is closed, means for generating a force that presses the sealing element against the seat, and means for limiting the extent of the sealing element motion when the valve is fully open. The sealing element must always be physically present as a distinctive part; other items from the above list may be realized by employing parts of the compressor or of the sealing element itself. For example, in a reed valve, which represents the simplest valve design, one finds only the sealing element as an individual part: the elastic force that keeps the valve at the seat is generated by the elasticity of the reed, the seat is machined into the cylinder head, and the stroke limiting is achieved by the bending resistance of the reed (Fig.1). This type of valve is commonly encountered in small refrigerating compressors for domestic use.

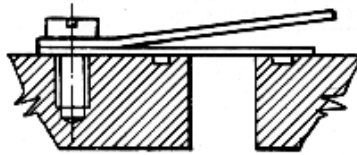


Figure 1: Simple reed valve

Large process compressors are equipped with valves of a more elaborate design, Referring to Fig. 2 below, in all three valve designs shown one finds the above mentioned four basic components realized as individual parts: the seat at the bottom, the sealing element with coil springs in the middle, and the stroke limiter at the top. They only differ in the type of the sealing element used; from left to right one sees a plate, concentric rings, and poppet. The plate valve shown has a sealing element made of reinforced plastic; a valve with a metal plate would normally also incorporate another metal plate whose function is to decelerate the sealing element on its way toward the stroke limiter, reducing thus the impact velocity on reaching the latter and increasing the chances for plan-parallel motion. The damper plate is normally not needed in metal plate valves used in small air compressors; the discussion shall henceforth be limited to such valves.



Figure 2: Common valve designs (from [45])

For the purpose of modelling, all valve designs without a damper plate can be abstracted to a configuration with a single sealing element depicted in Fig. 3 below.

In order to fully describe the operation of the valve, one must account for several states, events and processes that take place within the valve assembly. These are:

1. Valve in a closed state.
2. The opening event. When the force due to pressures acting upon the two sides of the plate overcomes the forces holding the plate at the seat, the valve begins to open and the gas starts flowing through the gap. Generally, there are three forces that oppose separation of the plate from the seat, these being the spring force, the stiction force due to a possible oil film at the contact surfaces, and the pressure force due to the unequal areas of the plate exposed to the respective pressures at the two sides of the plate.
3. Plate in motion between the seat and the stroke limiter, subjected to the spring force, the force due to the drag of the gas flowing past the plate, and the fluid friction opposing the motion (process).
4. Impact upon the stroke limiter. Note that there may be repeated impacts before the plate settles down.
5. Valve in a fully open state.

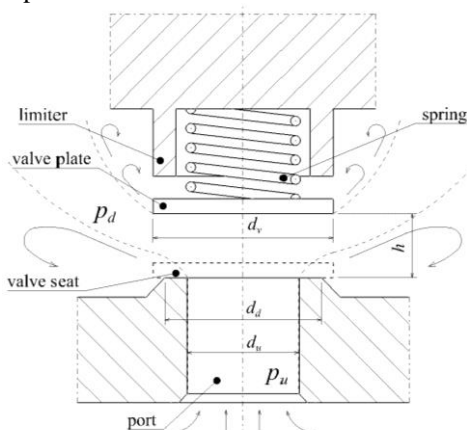


Figure 3: Generic model of a compressor valve

6. The detachment event. When the spring force prevails over the forces holding the valve open, the plate disengages from the stroke limiter. Similarly to the opening event, oil and/or gas stiction should be modelled (if present).
7. Plate in motion between the stroke limiter and the seat, same as Point 3 above.
8. Impact upon the stroke limiter. Note that there may be repeated impacts before the plate settles down.
9. Valve in a closed state.

2.3. VALVE FLOW MODELLING

Practically in all compressor performance prediction models, energy losses incurred at valves are modelled by measuring the performance of the valve in question on a test rig, and defining the so-called *discharge coefficient* as the quotient of the mass flow rate measured and a reference (ideal) value under the same flow conditions:

$$\alpha = \frac{\dot{m}_{\text{meas}}}{\dot{m}_{\text{ideal}}} = \frac{\dot{m}_{\text{meas}}}{\dot{m}_{\text{isen}}} \quad (1)$$

The reference component used is the ideal nozzle, having the same cross-sectional area at the throat as the valve being modelled. The true mass flow rate through the real valve is then

calculated by assuming isentropic expansion between the upstream and downstream conditions, and multiplying the ideal mass flow rate by the discharge coefficient. In reality, however, the (presumably) lower mass flow rate through the real device is caused by irreversibility, generating thus entropy in the flow process.

The discharge coefficient concept has its origin in the practice of flow rate measurement by means of standardized flow restrictions, such as e.g. orifices, nozzles, Venturi meters etc. [36]. In order to apply this concept to practical mass flow rate calculations, one must merely specify a suitable geometric cross-sectional area for the device in question, denoted by e.g. $A_{v,geo}$. Knowing the thermodynamic states at the device inlet and outlet, the actual mass flow rate in subsonic flow is calculated by invoking the well-known Saint-Venant-Wantzel equation of 1839:

$$\dot{m} = \alpha \cdot \dot{m} = \alpha \cdot A_{v,geo} \cdot \frac{p_{1t}}{\sqrt{R \cdot T_t}} \cdot \sqrt{\frac{2\kappa}{\kappa-1} \left(\Pi^{\frac{2}{\kappa}} - \Pi^{-\frac{\kappa+1}{\kappa}} \right)} \quad (2)$$

wherein $\Pi = p_{1t} / p_b$ stands for the inlet total (stagnation) to back (static) pressure ratio.

The isentropic part of the above formula refers to a reversible outflow from a pipe (hence the stagnation pressure and temperature terms) or a vessel; in the latter case the total pressure and temperature are replaced by their respective static quantities. The term to the right of the cross-sectional area represents the mass flux of the reversible outflow process under the thermodynamic conditions specified. It may be thought of as to result from a flow process taking place in an ideal nozzle, leading thus to the term *equivalent nozzle* for the reference element used.

The product of the discharge coefficient and the geometric cross-sectional area is referred as the *effective cross-sectional area* or *effective flow area* of the valve:

$$A_{v,eff} = \alpha \cdot A_{v,geo} \quad (3)$$

It should be borne in mind that the above formula set does not constitute a valve flow model in the sense of gas dynamics; it is merely a calculation device for arriving at the mass flow rate under given thermo dynamical conditions. However, discussing this subject is beyond the scope of the present paper; the interested reader is referred to e.g. [44] for further details.

Generally, the discharge coefficient for a given valve depends upon the geometric flow area and the pressure ratio across the valve. However, since the term under the square root of Eq. (2) has a maximum at:

$$\Pi_{crit} = [0.5(\kappa + 1)]^{\kappa/(\kappa+1)}, \text{ with } \Pi_{crit} = 1.893 \text{ for } \kappa = 1.4 \quad (4)$$

which is customarily referred to as the critical pressure ratio, and since it is an established fact (e.g. [6]) that compressor valves choke at much higher pressure ratios (up to 10), the above equation cannot be used as a mass flow rate model beyond the critical pressure ratio. The information as to the mass flow rate at overcritical pressure ratios must thus be supplied by the discharge coefficient, and this involves measurements and/or CFD studies.

There are flow model formulations, such as e.g. the Fanno flow theory [3], that take into account the effects of irreversibility in throttling flow upon the pressure ratio value at the onset of choking, but they have so far not been used in the compressor simulation practice.

3. VALVE DYNAMICS SUBMODELS

The dynamics of self-acting compressor valves was first considered in a systematic manner by Costagliola [14]. Although his model assumed stable behaviour of the sealing element, i.e. it did not allow for flutter, it provided a foundation upon which the majority of models developed in its aftermath were built. The developments up to 1972 were reviewed by MacLaren [30] and, somewhat later and in much more detail, by Toubert [39]. Bukac [12] attempted to present the entire field of valve dynamics and flow simulation in a compact manner, but his paper should be read as an overview, for it lacks arguments for choosing particular formulae and treats the flow calculation inconsistently in that a polytropic change is used simultaneously with the isentropic choking criterion. Habing [23] presents a modern view of the field and includes measurements to verify the theories used.

The only book devoted entirely to compressor valves was published by Böswirth [6], who has also been one of the most prolific authors in the field.

3.1. FORCE BALANCE AT THE OPENING EVENT

Using A_u and A_d to denote the respective upstream and downstream plate areas in contact with the seat, $F_{s,c}$ for the spring force in a closed valve and F_{adh} for the adhesion force, the valve is in a closed state when the following inequality is satisfied:

$$p_u \cdot A_u - p_d \cdot A_d \leq F_{s,c} + F_{adh} \quad (5)$$

whereby p_u corresponds to the cylinder pressure in the case of a discharge valve, and to the plenum (valve chamber) pressure in the case of a suction valve.

The valve starts opening when the inequality condition in Eq. (5) reverses, i.e.

$$p_u \cdot A_u - p_d \cdot A_d > F_{s,c} + F_{adh} \quad (6)$$

The opening process is strongly dependent upon the adhesion force in the contact area between the valve plate and the seat. If no liquid is present in the contact area the adhesion force may be due to molecular forces and/or under pressure; Toubert [39] uses the term "stiction" to refer to this phenomenon. He models the adhesion force by expressing it as an integral of the pressure distribution in the contact surface, i.e.

$$F_{adh} = \int_{A_c} (p_u - p) dA_c \quad (7)$$

Wherein A_c represents the contact surface area and p the pressure distribution function.

The situation is much more complicated if liquid is present in the contact area, which is always the case with lubricated machines and/or when liquid droplets are carried by the gas being compressed. Giacomelli and Giorgetti [20] considered this effect to be much stronger at the stroke limiter, which was also the opinion of Bauer [2]. The former authors [20] also measured the stiction force on a custom test rig, and found out that the shape of the stroke limiter surface has a strong influence upon the stiction force.

Khalifa and Xin Liu [26] concentrated on the suction valve stiction at the seat, and concluded that the primary reason for the stiction is the force arising from the oil film in the contact area being dilated in the opening process. Departing from the Reynolds equation of hydrodynamic lubrication

$$\frac{\partial p}{\partial r} = \mu \cdot \frac{\partial^2 u_r(z)}{\partial z^2} \tag{8}$$

where:

p - pressure variation in the film between the valve plate and seat,

r - radial coordinate of the oil film (meniscus), $R_{mi} \leq r \leq R_{me}$

R_{mi} - internal radius of the meniscus,

R_{me} - external radius of the meniscus,

h - distance of the plate from the seat,

$0 \leq z \leq h$ - axial coordinate,

$u_r(z)$ - velocity profile, and

μ - dynamic viscosity of oil,

they arrived at the following general equation:

$$F_{adh} = C \cdot \frac{\dot{h}}{h^3} \tag{9}$$

wherein the term C is referred to as stiction coefficient. Generally, the latter depends on the geometric features of the valve, and the viscosity of the liquid, e.g. oil, in the valve contact area. Several formulae for calculating the stiction coefficient are available in the literature; for illustration, we quote here two such formulae for the same physical configuration of the valve seat:

Table 1: Two formulae for the calculation of the stiction coefficient

Source	Stiction force of separation for raised flat valve seat and oil-starved gap
[1]	$C = \mu \cdot \left(\frac{d_d - d_u}{2} \right)^3 \cdot \frac{d_d + d_u}{2}$
[12]	$C = \frac{3 \cdot \pi \cdot \mu \cdot (r_B^4 - r_A^4)}{32} \cdot \left(\frac{r_B^2 - r_A^2}{(r_B^2 + r_A^2) \cdot (\ln r_B - \ln r_A)} - 1 \right)$ $r_A = \frac{d_u}{4} \cdot \left(1 + \frac{h_0}{h} \right) + \frac{d_d}{4} \cdot \left(1 - \frac{h_0}{h} \right)$ $r_B = \frac{d_u}{4} \cdot \left(1 - \frac{h_0}{h} \right) + \frac{d_d}{4} \cdot \left(1 + \frac{h_0}{h} \right)$

where h_0 stands for initial thickness of the oil film, and d_u and d_d are the inner and outer seat diameters, respectively (see Fig. 3).

In a most recent contribution to this area [35], the authors augment the model of Eq. 9 by introducing terms that take into account the curvature of the meniscus (capillary force), and the interfacial tension force. Upon comparing their formula with the one of Ref. [26] the authors state that their approach could not be validated due to the lack of experimental data.

3.2. FORCE BALANCE AT A MOVING VALVE PLATE

As soon as the valve begins to open the gas starts flowing through the gap between the plate and the seat, causing the upstream pressure at the former to diminish, which may in its turn

lead to a temporary closure of the valve. This may give rise to an alternation of the opening and closing events i.e. to the "bouncing" of the plate at the seat.

Denoting by h the distance of the plate from the seat, by F_s the spring force, by F_d the drag exerted upon the plate by the flowing gas, and by F_r the fluid friction force opposing the motion, one can write the instantaneous force balance at the plate as:

$$m_p \cdot \ddot{h} + F_r + F_s - F_d = 0 \quad (10)$$

which represents a general, single degree of freedom differential equation of the motion of mass m_p in the direction perpendicular to the valve seat.

Away from the seat and stroke limiter, damping of valve plate motion may be caused by friction forces acting upon the moving plate; in the vicinity of the seat and at the limiter, there are also the respective partially elastic impacts. The friction force is customarily modelled by assuming proportionality to the velocity \dot{h} of the valve plate [11][30][39]:

$$F_r = C_f \cdot \dot{h} \quad (11)$$

where C_f denotes the valve plate damping coefficient. Toubert [39] found that the same value of the damping coefficient applies to both the suction and discharge valves if they are of identical design and size, implying thus the former's independence on the gas density. Toubert also observed a weak dependence of C_f upon the oil content in the gas, and generally low values of the coefficient.

The same author [37] obtained a very reasonable agreement of experimental data and theoretical results by modelling the friction force as proportional to the spring load and acting in a sense opposite to the velocity \dot{h} of the valve plate. This empirical result could be explained to some extent by assuming mechanical friction at the spring surfaces which make a slight sliding action with respect to each other and to the valve plate when the latter is moving.

In most cases, valve spring force can be considered to be linearly dependent upon the deformation for the small distances over which a valve plate usually travels. The spring force is then given by:

$$F_s = k \cdot (h + h_0) \quad (12)$$

where k denotes the spring constant, h is the distance of the plate from the seat, and h_0 is the spring preload length. For a detailed analysis of the dynamic stresses in valve springs the reader is referred to [24].

Although Eq. (10) tacitly assumes that m_p represent the valve plate mass, one should also take into account the motion of the springs. Toubert [37] concludes that the inertial effect of the springs can be accounted for by adding an equivalent mass equal to one-third of the mass of the spring to the mass of the valve plate.

The force that gives rise to the plate motion, denoted by F_d in Eq. (10), and referred to as the drag or gas force, is the result of pressure distribution in the flow field around the valve plate. It is calculated as the area integral of the gas pressure load present at both sides of the valve plate, and customarily expressed as [19][39]:

$$F_d = C_d \cdot A_v \cdot (p_u - p_d) \quad (13)$$

where C_d denotes the drag coefficient, and A_v the valve plate area. In analogy with the effective flow area of Eq. (2), the product $C_d \cdot A_v$ is referred as the *effective force area*.

The drag coefficient is assumed to be constant for a given valve configuration, but as MacLaren [30] points out, this is rather not the case. Its value is determined empirically. However, Toubert [37] demonstrated a theoretical way to determine this coefficient by applying the momentum equation to a control volume enclosing the valve plate, obtaining:

$$C_d = \left[1 + \left(\alpha \cdot \varepsilon \cdot \frac{\pi \cdot d_v \cdot h}{A_u} \right)^2 \right] \cdot \frac{A_u}{A_v} - \frac{[\alpha \cdot \varepsilon \cdot (A_v - A_u)]^2}{A_v - A_u} \quad (14)$$

where α and ε denote the flow and expansion coefficients, respectively (see [39] for details).

Schwerzler and Hamilton [38] developed an analytical method to obtain the effective force areas by assuming incompressible flow, and arrived at equations that depended only on the geometry of the valves; the agreement with the measurements was good. Yuejin and Yongzhang [40] combined the theoretical and experimental studies, and concluded that their mathematical model of the drag coefficient was too complex and strongly dependent on the experimental data; they replaced it subsequently by a curve fit of the experimental data.

Valve plate and the associated springs constitute a potentially oscillating system; the excitation necessary to give rise to oscillations is provided by the interaction of this system with the flow. This phenomenon is referred to as flutter, and since it can lead to premature valve plate failures it was investigated by several researches in the field. In an early work by Upfold [43], experimental records of valve motion were used to arrive at design criteria a valve/spring system should fulfil in order to avoid flutter. In the notation of the present paper, an approximate relationship between design parameters and operation conditions of valve when oscillations or flutter of the inlet valve would not occur is defined as:

$$\omega \cdot p_u > \frac{k^{1.5} \cdot h_{\max}}{3 \cdot C_d \cdot A_v \cdot m_p^{0.5}} \quad (15)$$

where ω denotes rotational speed of the compressor, and h_{\max} is the maximal stroke of valve plate. According to the author [43], good design of inlet valves for reciprocating compressors would be to ensure that the value $\omega \cdot p_u$ is preferably never less than twice the calculated value of the parameter on the right hand side of Eq. 15.

Böswirth [11] formulated a theoretical model of valve flutter, and constructed an enlarged valve model that was installed into a suitable experimental device in order to verify the flutter model. Various effects, such as e.g. those of gas springs and inertia were studied, and a similarity theory was developed as an aid for understanding unsteady valve behaviour. Although only simple reed valves were dealt with in the study, the author considers that the know-how gained could also be brought to bear on other valve designs as well.

Often valve flutter is seen in conjunction with pressure pulsations in the piping. Although these are two quite different phenomena with possibility for mutual interference, there is a strong case for not neglecting the valve chambers and associated piping in the simulation of compressor performance, as already remarked in the General Considerations section of the present paper.

3.3. VALVE PLATE IMPACTS

Generally, impacts between the valve plate and the seat or stroke limiter give rise to stress concentration, leading to impact fatigue [34] which in its turn affects the service life of the plate. No generic modelling of the impacts seems to be possible, for the phenomena involved are rather complex. For example, it is questionable whether the classical impact between two solid bodies takes place in this case because, as the valve plate approaches either of the two limiting elements, it displaces the gas and oil present in the gap, adding thus a further mechanism to the impact process.

The valve plate is limited in its travel by the valve seat and in most valve designs by a limiter. It is assumed in the following that this limiter is fixed at an arbitrary distance from the seat and will not change its position when hit by the moving valve plate. When a moving body impacts at a fixed wall it will rebound with a velocity that is generally lower than the velocity before the impact. Only when its kinetic energy is absorbed or dissipated completely, it will remain in contact with the wall.

For the case that the valve plate rebounds, Habing [23] defines the so-called restitution coefficient as the ratio of the plate velocities immediately after (t^+) and before (t^-) the impact, i.e.

$$\left. \frac{dh}{dt} \right|_{(t^+)} = -e_{res} \cdot \left. \frac{dh}{dt} \right|_{(t^-)} \quad (16)$$

An impact is referred to as "fully elastic" when e_{res} equals 1, "inelastic" when $e_{res}=0$ and "semi-elastic" when $0 < e_{res} < 1$. Based on an analysis of his experimental results, Habing obtains $e_{res,s} = 0.3 \pm 0.1$ and $e_{res,l} = 0.2 \pm 0.1$ for the impacts of the valve plate at the seat and stroke limiter, respectively.

Performing a numerical investigation of the discharge valve dynamics with impact energy recuperation of 30%, which corresponds to a restitution coefficient of 0.55, Bukac [10] found almost negligible difference between hard stop and soft stop without oil on the valve lift and cylinder pressure. While the rebound from the stop has negligible impact on capacity, coefficient of performance (probably isentropic efficiency) and cylinder pressure, the rebound from the seat decreases compressor's capacity by 2.5% due to the flow-back of the gas.

3.4. VALVE IN FULLY OPEN STATE

A valve is fully open when the sum of forces holding the valve plate at the stroke limiter prevails over the spring force, which is expressed by the following inequality:

$$F_{s,o} \leq F_d + F_{adh} \quad (17)$$

The adhesion force may be due to oil stiction or the vacuum between the latter valve parts; the term $F_{s,o}$ represents the spring force when the valve plate is at the stroke limiter.

3.5. FORCE BALANCE AT THE DETACHMENT EVENT

Note that this event is not the counterpart to the valve opening; it can be understood as the onset of the valve plate motion toward the seat. The condition for this to take place is:

$$F_{s,o} \geq F_d + F_{adh} \quad (18)$$

After this event is completed, motion of the valve plate proceeds in accordance with the relationships derived in the previous section on valve plate motion.

4. VALVE FLOW CALCULATION

With reference to the formula set for the calculation of mass flow rate through discrete fluid ports presented in the Valve Flow Modelling section above (Eq. (1) to (4)), one should bear in mind that they are derived for steady flow. Since the flow through cylinder valves is unsteady at least with respect to time, it is customary to consider the flow as being steady at a given time instant, and changing without delay to a new value at a subsequent one. This constitutes the so-called *quasi-steady* approximation, which is found in the vast majority of performance prediction programs for IC engines and reciprocating compressors. In effect, this approximation is equivalent to neglecting valve dimensions in direction of flow.

The key term in Eq. (2) above is the discharge coefficient, for if its value is known, the mass flow rate through the valve is calculated in a straightforward manner. It is reasonable to expect that the discharge coefficient depends upon the valve geometry and the flow conditions; in the latter case, pressure ratio across the valve would be the main factor due to the choking phenomenon. Although the particular relationships between the discharge coefficient and the above mentioned quantities are obtained experimentally, Böswirth [8][6] convincingly demonstrated that fairly accurate approximations can be obtained through the application of the jet and boundary layer theories. His derivations also offer valuable physical insight into the flow phenomena in a compressor valve.

Böswirth's reports also contain experimental data for plate ring valve, which indicate that the strongest influence of the pressure ratio upon the discharge coefficient occurs at $1 < \Pi < 1.3$ and that the flow is choked for $\Pi \geq 3$. The author also introduces a different discharge coefficient which after the initial variation with pressure ratio, i.e. for $\Pi > 1.3$ remains essentially constant, but the pressure ratio term in Eq. (2) must be modified in order to use his discharge coefficient values. This is in line with the analysis of Blair [5], who insists that in dealing with the discharge coefficient the formula employed for the mass flow calculation must be inverted for the purpose of determining the discharge coefficient from the experimental data.

Measurements of valve flow are usually performed by fixing the valve plate at a given lift and varying the flow conditions, i.e. the pressure ratio. Data obtained in this manner are thus valid for a fully open valve; flow regime in a partially open valve is not adequately represented by these data. However, performing measurements with a normally configured valve, i.e. with a spring-loaded plate, is extremely difficult because of latent flow instabilities and is thus rarely performed.

Calculation of valve flow in the field of IC engines is still based on Eq. (2), i.e. on the cross-sectional area and the discharge coefficient being separated from each other. The trend in the compressor industry has been to use the effective flow area, probably because most of the studies deal with small refrigerating compressors which are rather similar to each other. In addition, the effective flow area is treated with the effective force area in the majority of studies. This makes sense, for there is a significant interaction between the two phenomena.

One of the first investigations of this kind is due to Schwerzler and Hamilton [38] who obtained good agreement between their theoretical predictions and the experimental data, although the former were derived by assuming incompressible flow in the valve.

Several other research teams used the concept of flow and force effective areas to determine the mass flow rate through the discharge and suction valves, as well as forces acting on the valve plate. Ferreira and Driessen [17] performed extensive measurements on different valves and presented the results obtained in non-dimensional form; in most cases they found much smaller variations of effective flow areas with the respective valve plate lifts than was the case with the corresponding effective force areas. Dechamps et al. [16] continued the above study and combined the measurements with numerical predictions under the conditions of laminar flow. Price and Botros [37] compared measured data with their numerical predictions of the effective flow area at low Reynolds numbers, and having obtained a good agreement proceeded to predict the former at high Reynolds numbers. They also found that the effective force area significantly varies with the lift. Kerpicci and Oguz [25] performed a CFD study of transient, i.e. unsteady, flow in leaf valves and found out that the discharge coefficient may be a function of the valve lift and pressure ratio, which Blair [5] also established in the case of IC engine valves. Recently, Murakami et al. [31] expressed the effective flow area as a surface plot in terms of the relative valve lift and the distance between the valve and the piston, and concluded that the simulation accuracy was better with the latter approach than with the model expressed in terms of valve lift only.

As already mentioned, an alternative to the calculation of mass flow rate by means of the discharge coefficient would be a model that explicitly takes into account the total pressure loss across the valve. For a general flow device with loss, the latter is expressed in terms of the *loss coefficient*, denoted by ξ and defined as:

$$\xi = \frac{p_{1,t} - p_{2,t}}{\left(\frac{1}{2} \cdot \rho \cdot u^2 \right)_{ref}} \quad (19)$$

where $p_{1,t}$ and $p_{2,t}$ stand for the total (stagnation) pressures at the inlet and outlet of the loss device, respectively, and the term in the denominator is the denormalizing dynamic pressure, taken at the inlet cross section. If the loss coefficient is expressed for an infinitesimal length and the resulting energy equation for compressible flow integrated between the inlet and the outlet, one obtains the so-called Fanno flow model [3]. Full discussion of such models is beyond the scope of this paper, but it is important to note that they, unlike the discharge coefficient concept, define the loss in a thermodynamically correct manner in that they relate the loss naturally with the entropy production as the ultimate loss metric [22].

Models based on the loss coefficient are used in the hydraulics, with an additional advantage of being augmented by vast collections of experimentally determined loss coefficient data for almost any device of importance for the practice. As to the reasons why this model class has not found application in the compressor simulation practice and, for that matter, in the area of IC engine simulation, the authors are of the opinion that it is the simplicity of Eq. (2), and the fact that the discharge coefficient concept has been the only one in use in the field of IC engines from the very beginning of their history. The latter has been especially

the case in the simulation models that incorporate one-dimensional gas dynamics methods to describe the wave action in the engine manifolds [4].

5. COUPLED SIMULATION OF VALVE DYNAMICS AND FLOW (FSI)

The quasi-steady valve flow calculation approach is justified for the cylinder and/or valve configurations with short channels; if the latter is not the case, the delays in the valve dynamics due to the inertia of the gas resident in the valve channels should be taken into account. Trella and Soedel [41] were among the first to treat this problem in a discharge valve; the model [41] was subsequently used to investigate the behaviour of the valve under different operating conditions [42]. Although the simulation results were not compared with measurements, the authors recommend the inclusion of the gas inertia effects into the valve calculation models, especially for fast-running compressors. Böswirth [9] performed a comprehensive theoretical analysis of the coupling between the gas and valve dynamics, and performed a series of measurements on a custom-built test rig [10]. With regard to the phenomenon of coupling, two main mechanisms were identified: gas inertia and unsteady work exchange between the flow and the valve plate; and the flutter was found to be affected by the so-called "gas spring effect". According to the author, replacing quasi-steady models by simplified unsteady models would constitute a small effort in comparison with gains in terms of simulation accuracy and understanding of the flutter phenomena. Habing [23] considered the unsteadiness in valve flow by augmenting the steady flow pressure loss formula by a transient flow term, and the already mentioned study of Kerpicci and Oguz [25] documents large differences between the quasi-steady and unsteady modelling approaches. Recently, after performing a CFD study of the fluid/structure interaction in a discharge valve, Link and Dechamps [29] state that "standard definitions of effective flow and force areas are not capable of describing mass flow rate and flow induced force in the opening and closing stages of the valve displacement". They rate their study is an initial step towards the understanding of flow inertial effects in compressor valves, and indicate the need for general correlations of effective flow and force areas for transient flow conditions.

6. SIMULATION RESULTS

In order to illustrate some of the concepts and models discussed above, simulation of a small air compressor with a 74 mm bore and 35 mm stroke was performed with a compressor simulation program that can also consider unsteady flow in the valve chambers and attached piping. The compressor is currently being experimentally investigated on a custom test rig for small air compressors in the Engine Laboratory of the Faculty of Engineering of Kragujevac, Serbia. The rig currently allows for recording several quantities of importance for evaluating thermo dynamical performance of the machine under test, such as cylinder pressure, exit mass flow rate, gas temperatures etc. Data recorded at an operating point characterized by the delivery pressure of 5 bar and the machine speed of 1000 rpm were selected for comparison with the simulation.

The machine obtains air through a small filter and approx. 50 mm of pipe from the laboratory, and delivers the compressed gas through 1.7 m of piping to an air-cooled heat exchanger. The model included all pipes up to the heat exchanger; due to the lack of the heat transfer data, the latter was modelled as a volume discharging the gas through a resistance to the environment. On account of the intricate construction of the cooler it was felt that a major part of the pulsations on the discharge side would be dissipated in the latter, obviating thus the need for including the rest of the piping in the simulation model. All cylinder walls were assumed to be adiabatic.

The valve simulation model consisted of the following sub models:

- Valve opening force balance without oil stiction, but with finite seat land area, i.e. $d_d \neq d_u$ (see Fig. 3)
- Calculation of the friction, spring, and drag forces per Eq. (11) – (13), respectively; the drag and friction force coefficients are assumed to be constant
- Valve plate impacts at the seat and stroke limiter per Eq. (16), and the restitution coefficient values within the bounds established by Habing [23]
- Valve mass flow rate calculation by means of the discharge coefficient model, as defined by Eq. (1) – (4)

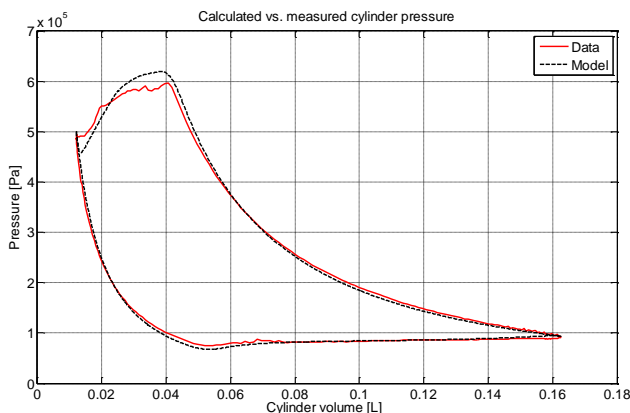


Figure 4: Calculated vs. measured indicator diagram for a small air compressor

Referring to Fig. 4, the calculated indicator diagram in terms of pressure is compared to the one obtained by averaging 40 measured cycles. In spite of the rather simple valve and cylinder models used, the agreement is satisfactory, with the exception of the discharge process, where one can claim a fair average agreement. Apparently, the discharge valve opens slower and remains open longer in the simulation as in the reality, indicating thus the need for model improvements. The valve lift traces of Fig. 5 suggest normal valve function at this operating point.

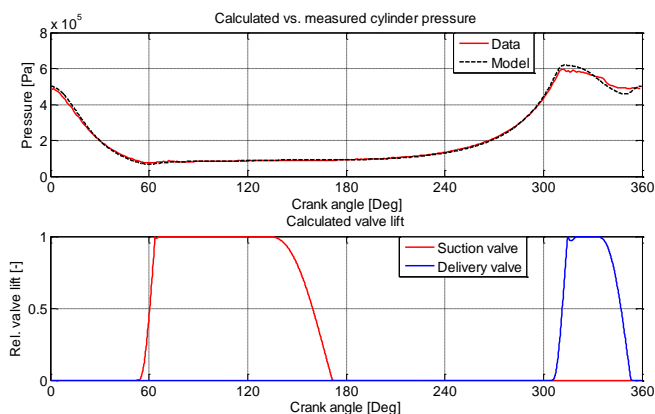


Figure 5: Pressure traces and calculated valve action for a small air compressor

7. CONCLUSIONS

The survey of the open literature presented in the paper shows that the modelling of valve dynamics is still a research subject. In spite of the ever increasing availability of the hardware and software for CFD and FSI simulations, these approaches are still neither practical nor developed enough in order to replace the one-dimensional models of the sealing element dynamics used heretofore. The latter, however, are in need of further improvement in some areas, such as establishing the variation of the drag force with the flow, considering the unsteady effects at small valve opening, refining the models of the resistance to valve plate motion, etc. This can be achieved by combining the measurements with the numerical methods, i.e. the CFD and FSI simulations.

Considering the valve mass flow rate calculation, it is felt that the research of the alternatives to the discharge coefficient concept should be actively pursued. The stagnation pressure loss model, which is thermodynamically sound and widely used in the hydraulics could represent a good starting point.

ACKNOWLEDGMENTS

The paper is a result of the research within the project TR 35041 financed by the Ministry of Science and Technological Development of the Republic of Serbia

8. REFERENCES

- [1] Aigner, R.: "Internal Flow and Valve Dynamics in a Reciprocating Compressor", PhD Thesis, Tech. Univ. Vienna, 2007.
- [2] Bauer, F.: "The Influence of Liquids on Compressor Valves", Proc. Purdue Compr. Conf., 1990, pp. 647-653.
- [3] Benedict, R.P. "Fundamentals of Gas Dynamics", Wiley-Interscience, 1982.
- [4] Benson, R.S.: "The Thermodynamics and Gas Dynamics of Internal Combustion Engines", Vol. 1 & 2, Edited by J.J. Horlock and D.E. Winterbone, Clarendon Press, Oxford, 1982.
- [5] Blair, G.P.: "An Alternative Method for the Prediction of Unsteady Gas Flow through the Internal Combustion Engines", SAE Paper 911850, 1991.
- [6] Böswirth, L.: "Strömung und Ventilplattenbewegung in Kolbenverdichtern", Published by the Author, Vienna, 2000.
- [7] Böswirth, L.: "Flow Forces and the Tilting of Spring Loaded Valve Plates, Part I", Proc. Purdue Compressor Conf., 1980, pp. 185-192.
- [8] Böswirth, L.: "Theoretical and Experimental Study on Fluid Flow in Valve Channels, Parts I and II", Proc. Purdue Compressor Conf., 1982, pp. 38-53.
- [9] Böswirth, L.: "A Model for Valve Flow Taking Non-Steady Flow into Account, Parts I and II", Proc. Purdue Compressor Conf., 1984, pp. 227-241.
- [10] Böswirth, L.: "Non Steady Flow in Valves", Proc. Purdue Compressor Conf., 1990, pp. 664-673.
- [11] Böswirth, L.: "Theoretical and Experimental Study on Valve Flutter", Proc. Purdue Compressor Conf., 1990, pp. 674-683.
- [12] Bukac, H.: "Understanding Valve Dynamics", Proc. Purdue Compressor Conf., 2002, Paper 1564.

- [13] Corberan, J.M., Gonzalvez, J.: "A Global Model for Piston Compressors with Gas Dynamics Calculation in the Pipes", Proc. Purdue Compressor Conf., 1998, pp. 851-856.
- [14] Costagliola, M.: "Theory of Spring-Loaded Valves for Reciprocating Compressors", Trans. ASME, J. Appl. Mech., Vol. 17, No. 4, 1950, pp. 415-420.
- [15] Cyklis, P.: "CFD Simulation of the Flow Through Reciprocating Compressor Self-Acting Valves", Proc. Purdue Compressor Conf., 1994, pp. 427-432.
- [16] Dechamps, C.J., Ferreira, R.T.S., Prata, A.T.: "The Effective Flow and Force Areas in Compressor Valves", Proc. Purdue Compressor Conf., 1988, pp. 104-111.
- [17] Ferreira, R.T.S. and Driessen, J.L.: "Analysis of the Influence of Valve Geometric Parameters on the Effective Flow and Force Areas", Proc. Purdue Compressor Conf., 1986, pp. 632-646.
- [18] Fleming, J.S., Shu, P.C., Brown, J. "The Importance of Wall Friction in the Compressible Flow of Gas through a Compressor Valve", Proc. Purdue Compressor Conf., 1988, pp. 195-197.
- [19] Fleming, J.S., Tramschek, A.B., Abdul-Husain, J.M.H.: "A Comparison of Flow and Pressure Distribution in Simple Valves Using Different Computational Methods", Proc. Purdue Compressor Conf., 1988, pp. 98-103.
- [20] Giacomelli, E., Giorgetti, M.: "Evaluation of Oil Stiction in Ring Valves", Proc. Purdue Compressor Conf., 1974, pp. 167-170.
- [21] Giacomelli, E. et al.: "Simulation of Cylinder Valves for Reciprocating Compressors", Proc. 8th Biennial ASME Conference on Engineering Systems Design and Analysis, 2006, Torino, Paper ESDA2006-95505.
- [22] Greitzer, E.M, Tan, C.S, Graf, M.B: "Internal Flow: Concepts and Applications", Cambridge Univ. Press, 2004.
- [23] Habing, R.A.: "Flow and Plate Motion in Compressor Valves", PhD Thesis, University of Twente, 2006.
- [24] Hatch, G. and Woollatt, D.: "The Dynamics of Reciprocating Compressor Valve Springs", Proc. Purdue Compressor Conf., 2002, Paper 1555.
- [25] Kerpicci, H. and Oguz, E.: "Transient Modelling of Flows Through Suction Port and Valve Leaves of Hermetic Reciprocating Compressors", Proc. Purdue Compressor Conf., 2006, pp. C122, 1-8.
- [26] Khalifa, H.E. and Liu, X.: "Analysis of Stiction Effect on the Dynamics of Compressor Suction Valve", Proc. Purdue Compressor Conf., 1998, pp. 87-92.
- [27] Leonard, S. M.: "Increase Reliability of Reciprocating Hydrogen Compressors", Hydrocarbon Processing, Jan. 1996, pp. 67-74.
- [28] Leray, D.: "Influence of Suction Valve Parameter on Volumetric Efficiency and Power Loss - Valve Design Chart", Proc. 7th Mache Int. Conf. on Compressors and their Systems, 2011, London, pp. 167-179.
- [29] Link, R. and Deschamps, C.J.: "Numerical Analysis of Transient Effects on Effective Flow and Force Areas of Compressor Valves", Proc. Purdue Compressor Conf., 2010, pp. 1319, 1-8.
- [30] MacLaren, J.F.T.: "Review of Simple Mathematical Models of Valves in Reciprocating Compressors", Proc. Purdue Compressor Conf., 1972, pp. 180-187.
- [31] Murakami, E., Link, R., Lajus Jr., F.: "Surface of Flow and Force Effective Areas Applied to Development of Reciprocating Compressors", Proc. Purdue Compressor Conf., 2010, pp. 1321, 1-6.
- [32] Ninkovic, D.: "Improving the Accuracy of Reciprocating Compressor Performance Prediction by Considering Real Gas Flow in the Valve Chambers and Associated

- Piping", Proc. ImechE7th European Congress on Fluid Machinery for the Oil, Petrochemical and Related Industries, The Hague, 1999, pp. 177-186.
- [33] Ninkovic, D.: "The Effects of Considering Unsteady Real Gas Flow in a Reciprocating Compressor Plant Model Upon the Accuracy of Performance Prediction", Proc. 1st EFRC Conference, Dresden, 1999, pp. 163-171.
- [34] Paczuski, A.W.: "Defining Impact", Proc. Purdue Compressor Conf., 2004, Paper 1718.
- [35] Pizarro-Recabarren, R., Barbosa, J.R., Dechamps, C.J.: "Modelling the Stiction Effect in Automatic Compressor Valves", Proc. Purdue Compressor Conf., 2012, Paper 1126.
- [36] Prandtl, L.: "Führer durch die Strömungslehre", F. Vieweg, Braunschweig, 1942.
- [37] Price, G.R. and Botros, K.K.: "Numerical and Experimental Analysis of the Flow Characteristics through a Channel Valve", Proc. Purdue Compressor Conf., 1992, pp. 1215-1225.
- [38] Schwerzler, D.D. and Hamilton, J.F.: "An Analytical Method for Determining Effective Flow and Force Areas for Refrigeration Compressor Valving Systems", Proc. Purdue Compressor Conf., 1972, pp. 30-36.
- [39] Touber, S.: "A Contribution to the Improvement of Compressor Valve Design", PhD Thesis, TU Delft, 1976.
- [40] Tramschek, A.B. and MacLaren, J.F.T.: "Simulation of a Reciprocating Compressor Accounting for Interaction between Valve Movement and Plenum Chamber Pressure", Proc. Purdue Compr. Conf., 1980, pp. 354-364.
- [41] Trella, T.J. and Soedel, W.: "Effect of Valve Port Gas Inertia on Valve Dynamics - Part I: Simulation of a Poppet Valve", Proc. Purdue Compressor Conf., 1974, pp. 190-197.
- [42] Trella, T.J. and Soedel, W.: "Effect of Valve Port Gas Inertia on Valve Dynamics - Part II: Flow Retardation at Valve Opening", Proc. Purdue Compressor Conf., 1974, pp. 198-207.
- [43] Upfold, R.W.: "Designing Compressor Valves to Avoid Flutter", Proc. Purdue Compr. Conf., 1972, pp. 400-406.
- [44] Ward-Smith, A.J.: "Internal Fluid Flow", Clarendon Press, Oxford, 1980.
- Yuejin, T. and Yongzhang, Y.: "The Experiment and Analysis of Drag Coefficient of the Ring Type Compressor Valve", Proc. Purdue Compressor Conf., 1986, pp. 623-631.
- [45] <http://www.belphie.nl/compart-compressor-technology/compressor-valves/>, accessed on June 28th 2012.

MVM Editorial Board
University of Kragujevac
Faculty of Engineering
Sestre Janjić 6, 34000 Kragujevac, Serbia
Tel.: +381/34/335990; Fax: + 381/34/333192
www.mvm.fink.rs